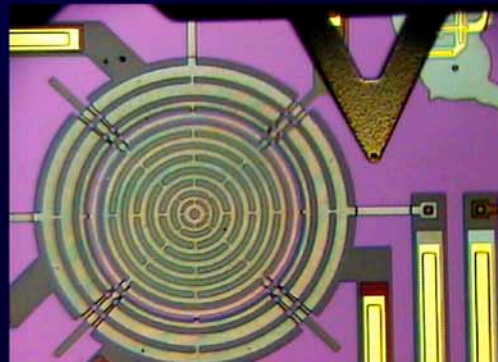
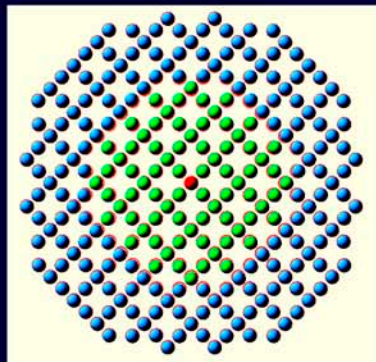
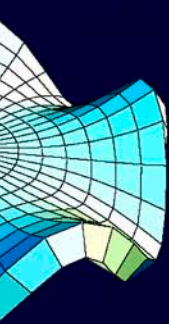


Materials Reliability Division

FY 2004 Programs and Accomplishments



MSEL

Material Science and Engineering Laboratory

NIST

**National Institute of
Standards and Technology**

Technology Administration
U.S. Department of Commerce

NISTIR 7125

September 2004

On the Cover:

Reliability of Modern Materials

Materials Reliability Division research focuses on reliability issues in structures on many scales. Advanced measurement and modeling methods are developed and applied to the characterization of materials properties. On a longer term, we also research the basic physics and materials science of failure. The images on the cover (from left to right) represent current research in:

acoustic characterization (a model of a vibrational mode in a sapphire disk), modeling of structure and properties from atomistic to continuum length scales (an atomistic model of a germanium “quantum dot” in silicon), MEMS-based measurement of mechanical properties on a cellular (biological) level, and biaxial measurement of strain in tissue.

**National Institute of
Standards and Technology**
Arden L. Bement, Jr.
Director

**Technology
Administration**
Phillip J. Bond
Undersecretary of
Commerce for Technology

**U.S. Department
of Commerce**
Donald L. Evans
Secretary



MATERIALS SCIENCE AND ENGINEERING LABORATORY

FY 2004 PROGRAMS AND ACCOMPLISHMENTS

MATERIALS RELIABILITY DIVISION

Alan F. Clark, Chief

Thomas A. Siewert, Deputy

NISTIR 7125

September 2004

Certain commercial entities, equipment, or materials may be identified in this document in order to describe an experimental procedure or concept adequately. Such identification is not intended to imply recommendation or endorsement by the National Institute of Standards and Technology, nor is it intended to imply that the entities, materials, or equipment are necessarily the best available for the purpose.

Table of Contents

Executive Summary	1
Technical Highlights	3
Targeted Workshops: Developing Strategies for the Future	4
The Structural Steel of the World Trade Center Towers	6
Quantitative Nanomechanical Properties	8
Pediatric Pulmonary Hypertension	10
Nanometrology	13
<i>Metrology for Nanoscale Properties</i>	
Metrology for Nanoscale Properties: Brillouin Light Scattering	14
Metrology for Nanoscale Properties: X-ray Methods	15
<i>Physical Properties of Thin Films and Nanostructures</i>	
Physical Properties of Thin Films and Nanostructures: Grain Size Effects on Actuator Fatigue	16
Physical Properties of Thin Films and Nanostructures: Nanoporous Low- κ Dielectric Films	17
Physical Properties of Thin Films and Nanostructures: Green's-Function Methods	18
<i>Applications of Carbon Nanotubes</i>	
Applications of Carbon Nanotubes: Carbon Nanotubes and Nanotube Contacts	19
Applications of Carbon Nanotubes: Cell Viability in Contact with Carbon Nanotubes	20
Applications of Carbon Nanotubes: Electrochemical Characterization of <i>In-Vivo</i> Neuronal Probes	21
Biomaterials	22
<i>Biomaterials Metrology</i>	
Biomaterials Metrology: Pediatric Pulmonary Hypertension	23
Biomaterials Metrology: Mechanical Response of Tissue Engineering Constructs	24

Table of Contents

Biomaterials Metrology: Cellular Level Measurements	25
Biomaterials Metrology: Quantitative Ultrasonic Characterization	26
Materials for Electronics	27
<i>Electronic Packaging and Components</i>	
Electronic Packaging and Components: Packaging Reliability	28
Electronic Packaging and Components: Acoustic Characterization	29
<i>Micrometer-Scale Reliability</i>	
Micrometer-Scale Reliability: Mechanical Behavior of Thin Films	30
Micrometer-Scale Reliability: Chip-Level Interconnects	31
Micrometer-Scale Reliability: Dynamic Imaging of Magnetic Domain Walls	32
Micrometer-Scale Reliability: Bridging Length Scales	33
Micrometer-Scale Reliability: Molecular Dynamics	34
Micrometer-Scale Reliability: Solder Reliability	35
Safety and Reliability	36
Infrastructure Reliability: Steel in the World Trade Center	37
Infrastructure Reliability: Test Methods for Fire-Resistant Steel	38
Infrastructure Reliability: Waveform-Based Acoustic Emission	39
Infrastructure Reliability: Charpy Impact Machine Verification	40
Materials Reliability Division FY04 Annual Report Publication List	41
Materials Reliability Division	45
Research Staff	46
Organizational Charts	49

Executive Summary

The **Materials Reliability Division's** mission is to develop and disseminate measurement methods and standards enhancing the quality and reliability of materials for industry. We have changed our portfolio of research projects slightly this past year as we have found new, critical technology gaps that limit the reliable use of materials. Yet we have maintained our competence in our core areas. Much of our research is concentrated in the NIST Strategic Focus Areas of Nanotechnology, Health Care, and Homeland Security. Our work covers a wide range of materials with a dimension span that extends from nanometer-scale devices, carbon nanotubes, and single cells, to tall buildings, gas pipelines and bridges. For FY04, we organized our research into the following focus areas:

Materials for Micro- and Optoelectronics

The U.S. microelectronics and related industries continue to face fierce international competition. The International Technology Roadmap for Semiconductors (ITRS) has long recognized the importance of metrology to the advancement of the industry by devoting an entire chapter to the subject. The 2003 ITRS calls specifically for solutions to the Interconnect Difficult Challenge (through 2009) of achieving necessary reliability due to the fact that "new materials, structures, and processes create new chip reliability (electrical, thermal, and mechanical) exposure. Detecting, testing, modeling and control of failure mechanisms will be key." We continue to support the industry through the following projects aimed at improved measurements, modeling, and advanced materials science: measurement of mechanical properties and micrometer-scale reliability of thin films; improved understanding of chip-level electrical and thermomechanical reliability in metallic interconnects; improved measurements and understanding of thermal flow and damage related to packaging and thin film reliability; linking models for structure and behavior of nanostructures from interatomic, to nano-, to continuum length scales; and molecular dynamics simulations of experimentally observed thin-film structure and behavior.

Nanocharacterization

Metrology, the science of measurement, plays a key role in the development and commercialization of nanotechnology. Manufacturing commercially viable nano-scale products, so widely envisioned in the press, demands vast improvements in our ability to measure material dimensions, characteristics, and structures at the nano-level. The overarching goal of our nanocharacterization effort is to develop reliable and accurate measurement techniques for a broad range of materials and material properties at the nano-scale. We are applying a variety of techniques to meet this challenge, such as atomic force acoustic microscopy (AFAM), Brillouin light scattering,

surface acoustic wave spectroscopy (SAWS), x-ray and electron diffraction, and multiscale modeling. We continue to explore synergies between these techniques as well as application of these measurement tools to a wide range of materials: ceramics, polymers, thin films, low-k dielectrics, self-assembled structures and others.

Biomaterials Metrology

The medical research community has recognized a burgeoning need to understand the role that the mechanical behavior of biological materials plays in normal and diseased tissues. This project addresses these needs on multiple length scales: cellular, cell plus matrix, and tissue levels. On the cellular level, we are using MEMS (microelectromechanical systems) devices to apply and measure loads and displacements on a single living cell. Techniques to calibrate the MEMS devices are being developed using an optical trap and the atomic force microscope. A novel bioreactor was developed to apply biaxial stress to tissue-engineered vascular grafts. Functionality is substandard if the grafts are cultured in a stress-free environment. Empirical models were identified that predict the compressive response of a porous scaffold used for tissue engineering. On the tissue level, work is ongoing to use a rat model to predict the mechanical response of arteries to the onset of pulmonary hypertension. Two models for inducing hypertension were compared. Complementary work was conducted using quantitative ultrasonic techniques. These physical acoustic techniques have also been applied to other tissue systems. Strong and diverse collaborations are growing with the University of Colorado, National Jewish Medical Research Center, Children's Hospital of Denver, and the Colorado School of Mines.

Infrastructure

The projects in this group are designed to develop measurement technology for determining a material's characteristics or for characterizing a measurement system. In FY04, we reduced our activities in lead-free solders, and transferred this effort to other infrastructure issues. The Charpy SRM program had over 900 customers in FY04, and we have shipped more than 1200 copies of our new training video in the past two years. A three-year international intercomparison of Charpy impact verification specimens was completed, confirming the equivalence of impact energy scales among the international producers of reference specimens. We finished measuring properties of steels used in the World Trade Center as part of the NIST-led study (report to be published in December 2004) and are looking at the issues that impede the use of fire-resistant steel. A joint proposal (with Metallurgy Division) on pipeline research was funded by DOT.

Al Clark, *Chief*
Tom Siewert, *Deputy Chief*

Division Chief's Commentary

Trying to advance our core science capabilities during the unusually tight budget of the 2004 fiscal year has been an extraordinary challenge for the Materials Reliability Division. The technical staff has risen to that challenge, and, in addition, they have reached out to increase our visibility and exposure to the outside world. This has taken the form of initiating and hosting several workshops, bringing in outside expertise to assess our program directions, and publishing in new journals and giving many invited talks. These extra and successful efforts are documented in this report along with the usual, high-quality technical achievements.

In my short time as Division Chief, I have been very impressed with the creativity and productivity of the Division staff and am pleased to have had the opportunity to work for them. "Reliability" has taken on a whole new meaning for me.

Al Clark
Chief
Materials Reliability Division

Technical Highlights

The following Technical Highlights section includes expanded descriptions of research projects that have broad applicability and impact. These projects generally continue for several years. The results are the product of the efforts of several individuals. The Technical Highlights include:

- Targeted Workshops: Developing Strategies for the Future
- The Structural Steel of the World Trade Center Towers
- Quantitative Nanomechanical Properties
- Pediatric Pulmonary Hypertension

Targeted Workshops: Developing Strategies for the Future

The Materials Reliability Division hosted two workshops in August 2004:

Computational Tools for Modeling Acoustic Propagation in Real World Materials.

Time-domain modeling of acoustic propagation is of interest to scientists and engineers involved in a range of disciplines such as medical ultrasound, material characterization, underwater acoustics, and geoaoustics. Real-world materials such as tissue, textile composites, and suspensions often exhibit properties that depend on the frequency of the interrogating sound and also lead to computationally intensive algorithms for modeling its acoustic response. Wider availability of high-performance computational tools will permit simulations of higher fidelity that benefit a range of industries involved in the modeling of acoustic propagation.

Reliability Issues in Nanomaterials.

Nanomaterials, with their promise of control over matter at the atomic level, are widely seen to offer the possibility of breakthrough products in fields from medicine to transportation to computers. This workshop reports a roadmap indicating metrology barriers, needs, and opportunities in nanomaterial manufacturability and reliability.

Kendall R. Waters, David T. Read, and Robert R. Keller

Acoustic Propagation

The Materials Science and Engineering Laboratory sponsored a two-day workshop (August 9–10, 2004) that was organized by the Materials Reliability Division with support from the Center for Theoretical and Computational Materials Science in an effort to propose collaborative investigations of problems in materials theory, modeling, and evaluation. The specific focus of the workshop was computational tools for modeling acoustic propagation in real-world materials with a broad goal of developing such tools for a wide audience. Specific topics addressed during the workshop included physical and mathematical models, computational techniques, high-performance computing (HPC) issues, and applications. Future plans include the development of a working group for HPC applications of acoustic propagation modeling.

Motivation

Many real-world materials exhibit acoustic propagation properties of attenuation and phase

velocity that depend on the frequency of the sound. These properties are not independent of one another and are known to be linked by the principle of causality. The consequences of causality for wave propagation have long been considered. The standard approach to this study is application of the Kramers–Krönig (K–K) dispersion relations, which place restrictions on the frequency response of a system. For the case of acoustics, the K–K relations can be used to relate the attenuation coefficient and the phase velocity.

More recently, interest has grown in the study of the time-domain consequences of causality-imposed restrictions. The basis for this approach is to consider a time-domain equivalent of the K–K relations, known as the time-causal relations. These relations are used to modify a lossy wave equation to include effects due to the frequency dependence of phase velocity, commonly referred to as dispersion. The inclusion of frequency-dependent attenuation in time-domain models is straightforward. However, the effects of dispersion depend on the history of the acoustic pressure field, and its inclusion in time-domain models can be computationally intensive.

A standard numerical approach for time-domain modeling of acoustic propagation employs a finite-difference time-domain (FDTD) technique. FDTD code has long been used for electromagnetic wave propagation and is becoming more widely used for acoustic wave propagation. Similar to analytical modeling of acoustic propagation, numerical modeling of materials with loss and dispersion is non-trivial. At present, the availability of such a FDTD code that accounts for loss and dispersion is limited.

Participation

The workshop was organized in collaboration with colleagues Drs. J. Mobley and K. Wallace of the U.S. Army Research Laboratory (ARL) and Washington University in Saint Louis, respectively. Invited speakers included Dr. D. Marlin of the U.S. ARL, Dr. G. Norton of the U.S. Naval Research Laboratory, Dr. M. Rielly of Philips Medical Systems, and Dr. T. Szabo of Boston University. These speakers provided reviews of the modeling and HPC aspects of acoustic propagation in various acoustical systems. Contributing speakers and other participants provided discussions on specific applications such as surface acoustic waves in thin films and medical ultrasound contrast imaging. These participants came from an equally diverse range of institutions including the National Oceanic and Atmospheric Administration, the University of Colorado, The Children's Hospital in Denver, and Weidlinger Associates Inc., as well as NIST.

In addition to presentations, break-out sessions were held to discuss in more detail common aspects of the physical and mathematical models for different acoustic environments and issues related to HPC. The establishment of a working group for continued collaborations was discussed and is actively being pursued. A summary of the workshop will be prepared and distributed in the near future.

Nanomaterials Reliability

The Materials Reliability Division of NIST, the University of Colorado, and the National Science Foundation have teamed to offer the Workshop on “Reliability Issues in Nanomaterials,” held August 17–19, 2004.

Motivation

Nanomaterials, with their promise of control over matter at the atomic level, are widely seen to offer the possibility of breakthrough products in fields from medicine to transportation to computers. NIST is a participating agency in the National Nanotechnology Initiative; one of NIST’s key roles is to develop metrology and tools needed for the success of nanotechnology. But NIST cannot do this alone; the nation will be best served by a cooperative effort, at a pre-competitive level, among all interested parties.

Goal

The goal of this workshop, inspired by the success of the International Technology Roadmap for Semi-conductors, was to produce a first version of a roadmap including: (i) present state-of-the-art in nano-mechanical reliability research, including experimental, theoretical, and numerical approaches; (ii) identification of measurement-related barriers to improve reliability; and (iii) identification of possible solutions or approaches to solutions, which overcome such barriers. The report of the workshop, describing our progress toward defining a nanomaterials reliability roadmap, will be published as a NIST Special Publication.

Technical Focus

The nine plenary presentations were divided into two main areas: fabrication and processing; and characterization and testing. General topics of interest included:

- Nanomaterials processing and fabrication, and their effects on mechanical reliability;
- Methods and techniques for characterizing structure of nanomaterials;
- Methodologies for measuring mechanical properties in nanomaterials;

- Experimental and modeling approaches to understanding effects of structure and dimensional scaling on mechanical behavior of nanomaterials, with emphasis on surface and interface issues;
- Approaches to understanding what roles nano-mechanics plays in other types of reliability; and
- Structure, property, and lifetime prediction.

This workshop addressed some of the issues raised during the Nanomechanics Breakout Track of the NNI Interagency Workshop on Instrumentation and Metrology, held January 2004 at NIST–Gaithersburg. Namely, we addressed the following Grand Challenges:

- Modeling of nanomechanical experiments;
- Integration of multiple techniques for measurement and characterization;
- Experimentation/testing under real application conditions;
- Standardization and calibration;
- Instrument development for nanomechanics;
- High-throughput, automated nanomechanics measurements.

Participation

The eight non-NIST plenary speakers were: Susanne Arney (Lucent Technologies), John Randall (Zyvex), Ken Rodbell (IBM), Rachel Goldman (Univ. of Michigan), William Gerberich (Univ. of Minnesota), Martin Dunn (Univ. of Colorado), Nancy Burnham (Worcester Polytechnic Institute), and Neville Moody (Sandia National Laboratories). Each was allotted 60 minutes for presentation and discussion. We invited 50 additional participants representing industry, national laboratories, and universities. Breakout sessions followed for in-depth discussion of metrology needs for advancing the use of nanomaterials in practice.

The ninth plenary session featured a presentation of ongoing nanomaterials research in the NIST Materials Science and Engineering Laboratory by Doug Smith (MSEL/Ceramics Division) and included discussion of the role of NIST. This was followed by a summary of the technical presentations and discussion of priorities for future mechanics-related nanomaterials research by all the organizations represented.

For More Information on this Topic

K.R. Waters, D.T. Read, R.R. Keller (Materials Reliability Division, NIST)

The Structural Steel of the World Trade Center Towers

In August of 2002, NIST took responsibility for the investigation of the World Trade Center disaster. The investigation objectives include determining: why the buildings collapsed; the procedures and practices used in the design, construction, operation and maintenance of the buildings; and areas in codes and practices that warrant revision. The eight interdependent projects include Project 3 — Analysis of Structural Steel, led by the Materials Science and Engineering Laboratory. The objective of the project is to determine and analyze the properties and quality of the steel, weldments, and connections from steel recovered from the World Trade Center.

Stephen W. Banovic, Richard J. Fields, Timothy J. Foecke, William E. Luecke, J. David McColskey, Christopher N. McCowan, Thomas A. Siewert, and Frank W. Gayle

In terms of the steel used, the World Trade Center was very complex. Plans called for steels of fourteen different yield strengths between 36 ksi and 100 ksi. Many of these steels were proprietary and were not supplied to any existing ASTM specification. To further complicate matters, four different fabricators provided steel for the upper stories, and each used steel from more than one supplier. Most of the records that documented the steel actually used were either not preserved or destroyed in the collapse.

The MSEL Metallurgy and Materials Reliability Divisions have determined properties of the steel recovered from the WTC site and characterized failure modes associated with pre-collapse damage. This information has been provided for use in models of the building response to airplane impact and fire. In 2004, all major tasks were completed.

Task 1 — Collect and Catalog Physical Evidence

The Structural Engineers Association of New York (SEAoNY), later supplemented by NIST personnel, spent countless hours selecting steel in the New Jersey recycling yards for later forensic analysis. After shipment to NIST, the Metallurgy Division cataloged the 236 recovered steel components. Since many pieces were stamped and painted with unique serial numbers correlated with the building plans, it was often possible to identify the exact original location in the building.

As a second part of this task, we also researched contemporaneous construction documents and steel specifications. This task helped identify steel suppliers and fabricators, as well as material substitutions.

Task 2 — Categorize Failure Mechanisms Based on Visual Evidence

The damage to the steel components of the buildings represents an important check on the accuracy of the fire and impact modeling, with the caveat that the recovered steel could have been damaged before the collapse, during the collapse, or during the salvage efforts.

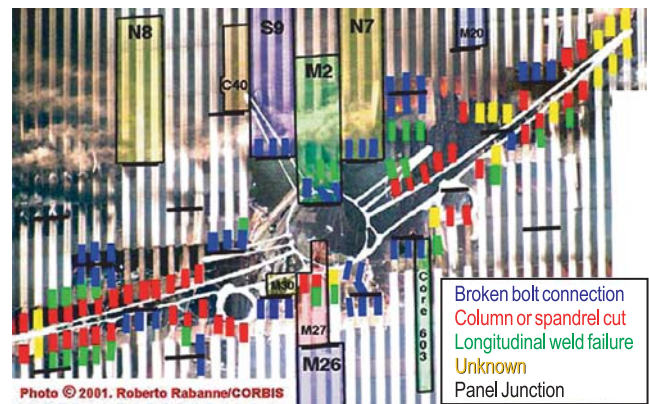


Figure 1: Enhanced image of the impact zone has allowed determination of failure modes in the perimeter columns. An outline of the plane is superimposed. Steel panels recovered for the investigation are highlighted in color.

Image enhancement techniques were used to study photographs of the impact zones of the towers to establish the failure mechanisms of the perimeter columns. By making montages of many different images, it was possible to produce a nearly smoke-free, composite view of the columns that the aircraft struck. The columns failed by several different mechanisms. One important result was the demonstration that several key impact-zone columns in the NIST inventory were damaged primarily in the aircraft impact, and not in the subsequent collapse or recovery efforts. Figure 1 is a map of the impact zone of WTC 1 that illustrates the nature of the damage to the individual columns.

Tasks 3 & 4 — Determine Steel Properties to Support Airplane Impact and Structure Performance Studies; Correlate Properties with Those Specified in the Construction

One important part of this task was to assess the quality of steel and determine whether it met the original specifications. In support of this goal, the group conducted more than 200 room-temperature tensile tests on samples from 39 different building components, which represented

all the steels relevant to the investigation. Tests indicate that the steels generally met or exceeded the specified minimum strengths (Figure 2).

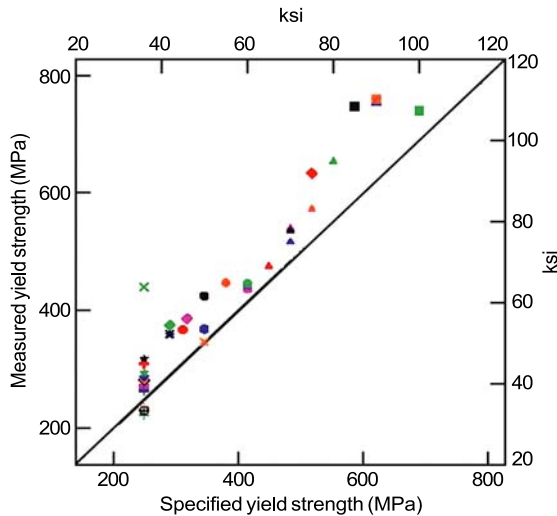


Figure 2: Yield strength — measured vs. specified minimum. The few anomalous data can be attributed to damage incurred in the collapse that removed the yield point behavior, or to the natural and accepted strength variability of structural steel.

Steel specifications also regulate the chemical compositions. More than 350 different specimens, representing nearly every relevant steel component in the building, were analyzed for chemical composition and all of the sections relevant to the investigation. The chemical analysis helped confirm archival information that an American steel mill supplied steel for parts of the perimeter columns. The analyses also support the conclusion that the steels in the buildings met the specifications called for in the building plans.

The strength of steel increases as the deformation rate increases. Accurately modeling these rate effects is essential for estimating the energy and momentum of the aircraft remnants which damaged the core columns. To establish the strain rate sensitivity of the relevant steels, we have conducted more than 100 tests on specimens from both the perimeter and core columns at rates up to 2000 s^{-1} (200,000 % deformation per second).

Ultimately, the fires in the towers weakened the steel structure leading to collapse. We conducted more than 100 high-temperature tensile and creep tests to provide models of the deformation of structural steel at elevated temperatures for use in models of the building response to the fires.

Task 5 — Analyze Steel to Estimate Temperature

Just as the nature of the deformation and failure of the recovered steel reveals information about the

impact and collapse, the steel can also contain evidence of its exposure to the elevated temperatures in the fire. The situation is made more complex because much of the steel was also exposed to extended fires in the rubble before recovery. Several different methods, both conventional and novel, were examined for estimating high-temperature excursions seen by the steel. Only one method proved to be robust and easy to implement: paint on steels that reached temperatures over $250\text{ }^{\circ}\text{C}$ cracked from the difference in thermal expansion between the paint and the steel.

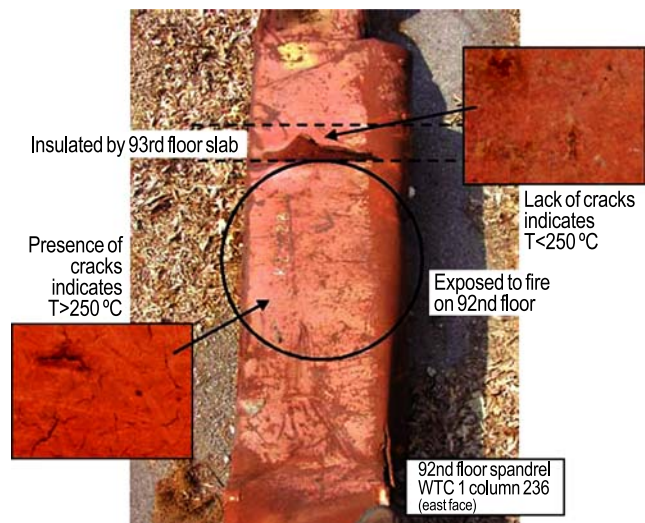


Figure 3: Illustration of the method to establish the temperature excursions of recovered steel. The segment of the column protected by the floor slab remained at lower temperature.

From photographs showing fire in windows, all recovered columns that may have been exposed to pre-collapse fire were identified and characterized using the paint crack technique. Figure 3 illustrates one of the columns that showed evidence of having exceeded $250\text{ }^{\circ}\text{C}$.

Outputs

Outputs for the project include parts of the June 2004 *Progress Report on the World Trade Center Disaster* (NIST SP 1000-5) and numerous memos for contractors that explain how to employ Project 3 data and deformation models. The final NIST investigation report will be released in the spring of 2005.

For More Information on this Topic

T.A. Siewert (Materials Reliability Division, NIST);
F.W. Gayle (Metallurgy Division, NIST)

Quantitative Nanomechanical Properties

We are developing AFM-based metrology for rapid, nondestructive measurement of mechanical properties with true nanoscale spatial resolution. Atomic force acoustic microscopy methods enable elastic-modulus measurements at either a single point or as a map of local property variations. Complementary information obtained with scanning electron microscopy provides insight into structure-property relations and helps to interpret nanoscale contact-mechanics behavior. The information obtained furthers our understanding of the nanomechanical properties of surfaces, thin films, and nanoscale structures.

Donna C. Hurley

New measurement solutions are required to address the rapidly burgeoning field of nanotechnology. In particular, information about mechanical properties on the nanoscale is needed. Knowledge of properties like elastic modulus and interfacial quality (defects, strain, adhesion, etc.) is critical to successful development of new films and nanoscale assemblies. Such information could also assess integrity or reliability in applications from microelectronics to biotechnology. Existing methods for mechanical-property measurements have drawbacks: they are destructive, limited to specialized test specimens, or not quantitative. Instrumented or “nano-” indentation (NI), a current industry workhorse, will have limited value as scales shrink well below 1 μm , and softer materials are more frequently used.

To meet this need, we are developing tools that exploit the spatial resolution of atomic force microscopy (AFM). Our approach, called atomic force acoustic microscopy (AFAM), involves the vibrational resonance of an AFM cantilever when its tip is in contact with a sample. By comparing the cantilever’s contact-resonance frequencies for an unknown material to those for a reference sample with known properties, the indentation modulus M of the unknown material can be determined. [For an isotropic material $M = E/(1-\nu^2)$, where E is Young’s modulus and ν is Poisson’s ratio.] The small tip radius ($\sim 5\text{--}50$ nm) means that we can obtain *in-situ* elastic stiffness images with nanoscale spatial resolution.

In FY04, we extended our quantitative AFAM techniques in a variety of ways. In one effort, the effect of film thickness on measurement accuracy was investigated. We measured M for three nickel (Ni) films approximately 50, 200 and 800 nm thick. The values of M ranged from 220 GPa to 223 GPa, significantly lower than that expected for bulk

polycrystalline Ni. Scanning electron microscopy (SEM) revealed that the films were nanocrystalline (grain diameter < 30 nm). The observed reduction in M may be attributed to an increased volume fraction of grain boundaries in the nanocrystalline films. More importantly, the average values of M for all three films were the same within measurement uncertainty ($\sim 10\%$). Thus the AFAM results were not influenced by the elastic properties of the silicon substrate, even for a 50 nm film. This behavior is due to the fact that the AFAM stress field extends less than 100 nm into the sample and decreases rapidly with depth due to the small applied static loads (0.3–3 μN) and small radius of contact (5–25 nm). Our result contrasts sharply with nanoindentation, in which substrate properties must be included to accurately measure submicrometer films.

The elastic properties of the 800 nm Ni film were also measured using NI, microtensile testing, and surface acoustic wave spectroscopy (SAWS). Both AFAM and NI measure the film’s out-of-plane indentation modulus. The results were in excellent agreement, validating AFAM as a quantitative method in spite of its relative newness. Microtensile testing values for the in-plane Young’s modulus of the film were not consistent with the AFAM and NI results if the film was assumed to be elastically isotropic. The apparently contradictory results were reconciled by use of a transversely anisotropic model for the film’s elastic properties. This model is consistent with the strong $\langle 111 \rangle$ film texture observed by x-ray diffraction. When analyzed with the same model, the SAWS results indicated that the film density was only slightly lower ($< 5\%$) than the bulk value. These results illustrate a relatively straightforward way to interpret mechanical-property measurements of thin films that is based on a more physically realistic model than the simple assumption of elastic isotropy.

Another effort investigated the effects of relative humidity (RH) on AFAM measurements. AFAM contact

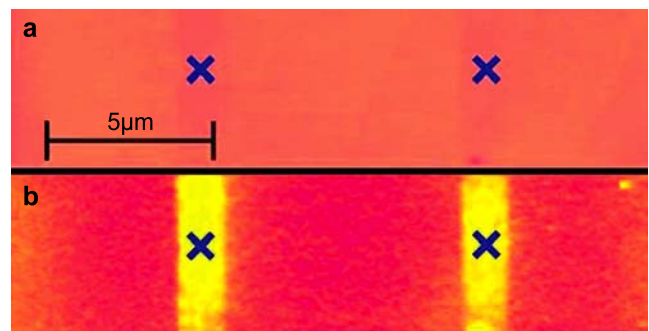


Figure 1: a) AFM tapping-mode topography and b) AFAM relative-stiffness images of Si with *n*-octyldimethylchlorosilane SAM.

stiffness measurements may be affected by a variable water layer between the tip and sample, at least in some cases. By refining our data analysis methods to include the effects of such a layer, apparent correlations between the measured values of M and the ambient RH were eliminated. This year we also developed a RH-controlled AFM chamber in order to systematically study these effects. Samples for the experiments were provided by the Polymers Division and consisted of patterned self-assembled monolayers (SAM) of n-octyldimethylchloro-silane on Si substrates. Through controlled ultraviolet-ozone exposure, the relative hydrophobic/hydrophilic nature of the SAM was adjusted in different sample regions. Figure 1 shows an AFM topography image and an AFAM relative-stiffness image for a SAM/Si sample. The SAM stripes are virtually invisible in the topography image, even at very high resolution (10 nm full scale height). However, the AFAM image clearly reveals the hydrophobic SAM stripes. The regions covered by the SAM appear more compliant (lower contact stiffness) due to AFAM's sensitivity to local variations in the tip-sample adhesion. We are currently performing further experiments on similar samples in order to quantify how humidity and adhesion effects can be distinguished from true mechanical-property variations.

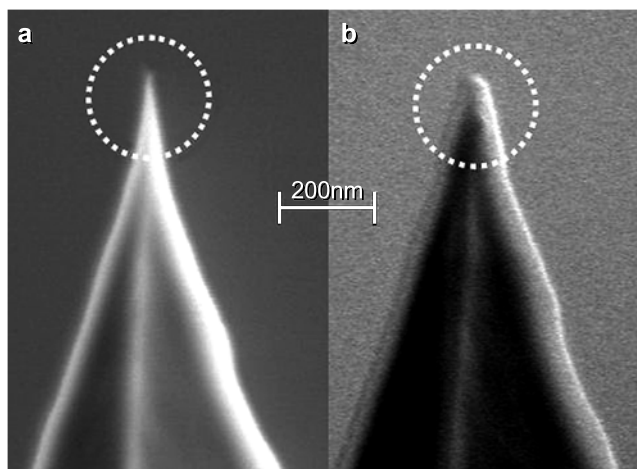


Figure 2: SEM images of AFM cantilever tip a) before use and b) after repeated AFAM contact experiments. The circled regions indicate the tip wear that occurred through use.

AFAM contact-resonance frequencies depend not only on elastic properties, but also on the value of the tip radius R . Thus knowledge of R and how it changes over time is essential for accurate measurements of elastic properties. To address this issue, we performed AFAM experiments with different AFM cantilevers on a sample with known elastic properties. The first

measurements were done at relatively low static loads; the load was then successively increased up to several micronewtons to try to break and/or plastically deform the tip. High-magnification SEM images were obtained before and after each AFAM measurement. As can be seen in Figure 2, R increased with use, indicating tip wear. Values of R measured from the SEM images were compared to the values obtained from AFAM data using a Hertzian contact-mechanics model. The AFAM values of R were consistently smaller than the SEM values. Further data analysis and additional experiments are planned to clarify this issue. The knowledge gained in this way will help us to refine our understanding of AFAM contact mechanics, beyond the Hertz approximation, in order to improve measurement accuracy and repeatability.

In related work, we are performing finite-element studies of the AFM cantilever. The finite-element mesh is based on actual cantilever dimensions from SEM images and includes elastic anisotropy. The predicted free-space resonant frequencies are in excellent agreement with those observed experimentally. Work is underway to predict the vibrational behavior in contact. These results will allow us to refine our data analysis models and thus improve measurement accuracy.

The research described above involves either *quantitative single-point* measurements, or *qualitative imaging* of relative stiffness. In FY04, we worked to realize our ultimate goal of *quantitative nanomechanical mapping*. Critical to our success is a new frequency tracking circuit that can determine the contact-resonance frequencies at each image pixel. The circuit is based on digital signal processing architecture that enables rapid data acquisition (typically < 30 min. for a 256×256 image). We have begun to obtain resonance-frequency images for a variety of materials. Recent enhancements to our AFM mean that we can acquire images from not only the flexural modes, but also the torsional modes of the cantilever. By combining information from flexural and torsional images, it may be possible to determine simultaneously both Young's modulus and Poisson's ratio for an isotropic material. Work in upcoming months will focus on issues related to quantitative image interpretation such as calibration procedures, cantilever selection, tip wear, and choice of contact-mechanics model. Each of these elements plays a role in attaining our goal of truly quantitative nanomechanical imaging.

For More Information on this Topic

D.C. Hurley (Materials Reliability Division, NIST)

Pediatric Pulmonary Hypertension

Pulmonary hypertension is a potentially fatal complication of congenital heart defects in children who live at high altitudes. Discovering the pathophysiology and expression of the disease may open the way to finding new, more effective diagnostics and treatments. Our contribution to this goal is to investigate the differences in the mechanical properties of the pulmonary artery and its constituents between healthy and diseased tissue.

Elizabeth S. Drexler

Members of the Biomaterials Metrology Project are working in conjunction with researchers at the University of Colorado and Children’s Hospital of Denver to characterize the development and pathophysiology of secondary pulmonary hypertension (PHT) in children. The high elevation of the Rocky Mountain region causes children born with heart defects to have a greater propensity for developing PHT, so it is an area of great concern for this region. Members of this collaborative team are addressing the role of fluid mechanics, biochemistry, pathology, histology, and the arterial wall mechanics during development and at maturation of the disease. It is our goal to develop new, less-invasive diagnostics that might hasten treatment and mitigate permanent damage. At the present time, diagnosis is sometimes delayed by two factors: a variety of conditions that can display similar clinical expression, and the reluctance of physicians to subject a child to catheterization unless it is clearly necessary.

The Pediatric Pulmonary Hypertension subproject is focusing on the dual goals of quantizing the mechanical properties and identifying the structural differences between normotensive and hypertensive pulmonary arteries (PAs). Our approach is to begin with a rat model to determine whether we can detect differences in the stress–strain and ultrasonic properties between conditions. We have chosen the Long–Evans breed of rats because they can be genetically modified so that the endothelin B receptor is disabled (knock-out or KO). The endothelin B receptor is responsible for activating the vasodilators prostacyclin and nitric oxide.

The test matrix includes testing controls (otherwise referred to as untreated wilds), monocrotaline-treated wilds, hypoxic wilds, hypoxic KOs, and perhaps monocrotaline-treated KOs. Monocrotaline is a synthetic chemical derived from a naturally occurring substance that produces an inflammatory response in the lungs that

typically degenerates into PHT. The rats are injected with monocrotaline subcutaneously, and the disease is allowed to develop over four weeks before the arterial tissue is tested. To induce PHT with hypoxia, rats are held in a hypobaric chamber that simulates oxygen conditions at 5200 m above sea level for three weeks before testing. Specimens from the trunk, and the right and left main branches are tested. It is thought that these proximal arteries are likely to be used for clinical diagnosis as they are more readily imaged non-invasively.

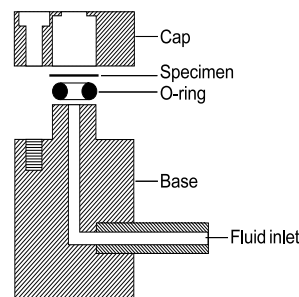


Figure 1: Schematic of the bubble test fixture.

A bubble-test configuration is employed to obtain stress–strain data (Figure 1). The specimen sits in a reservoir and is pressurized in 1.4 kPa (10 mm Hg) increments from the adventitial side with a physiological solution. Images of the bubble profile are collected at each pressure increment from six camera angles located 30° apart. These images are used to measure the changing length of the extruded bubble to calculate strain. The bubble is fitted as an ellipsoid to calculate the surface area to determine stress. The various camera angles allow us to account for anisotropic deformation. However, at this point, we are using the formulation for the stress at the apex of an ellipsoid of an isotropic material to approximate the stress. Models are nearing completion that will determine the elastic constants of the material from the experimental measurements based on established anisotropic constitutive relationships.

The results of the tests for each population are shown in Figures 2a–d. All values for strain were relative to the displacement measured at 1.4 kPa. Both the hypoxic wilds and the hypoxic knock-outs showed less strain at a given stress value than did the controls — the knock-outs more so than the wilds. It should also be pointed out that, in general, the hypoxic specimens were pressurized to equivalent pressures to the controls and monocrotaline treated specimens, and oftentimes 15–20 % higher. The thickness of the hypoxic specimens had a dramatic effect on the stress relationship. We found that the effect of the monocrotaline treatment on the wild population was

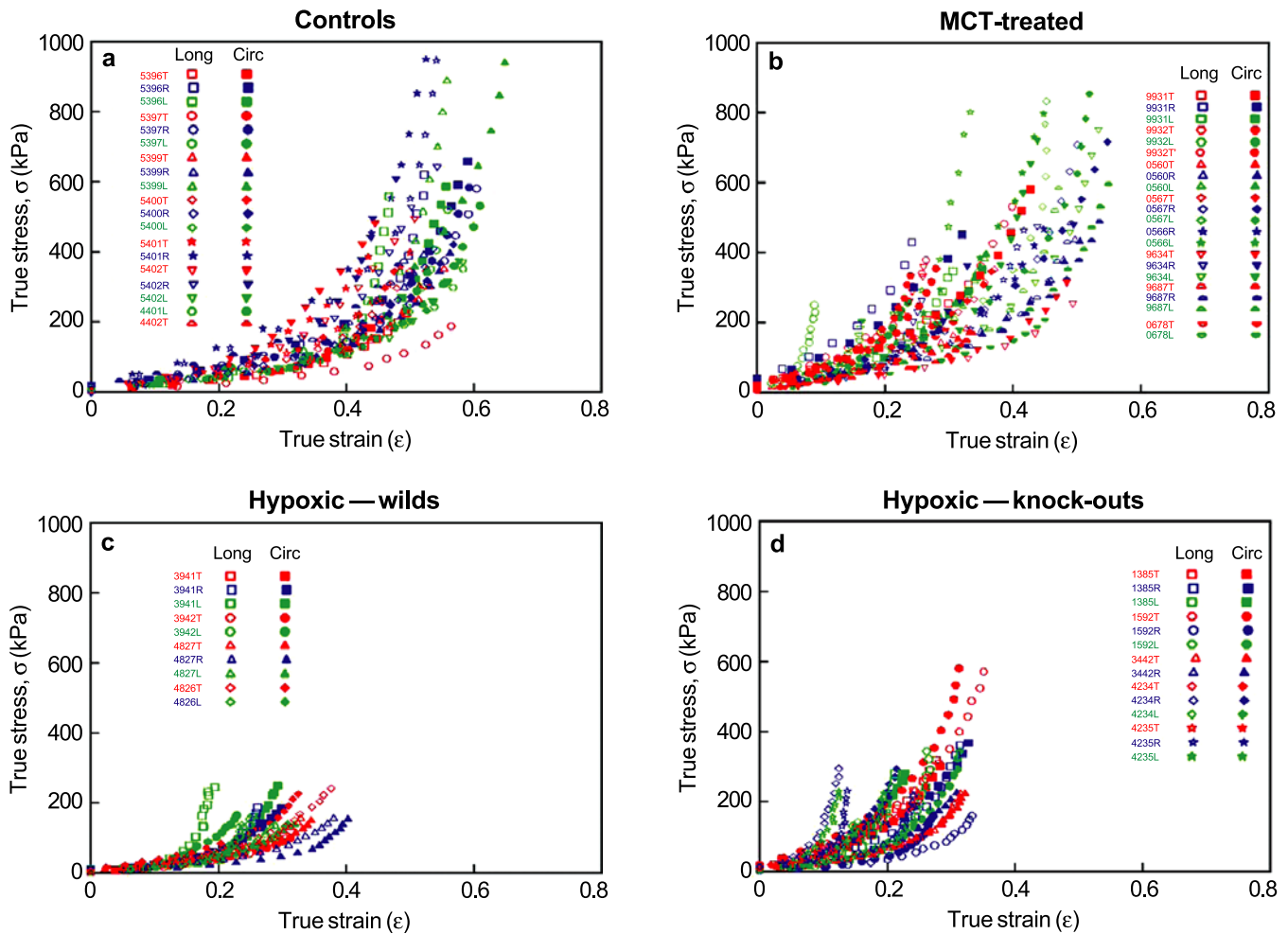


Figure 2: Stress–strain results from the a) control, b) mono-crotaline-treated, c) hypoxic wild, and d) hypoxic knock-out rats.

unclear on the stress–strain relationship. We are in the process of identifying a reasonable mathematical model for the data so that statistical analyses may determine significance among the populations. Work has begun to correlate general trends in our pressure–displacement data to *in vivo* compliance data acquired by use of input impedance measurements in the catheterization laboratory.

Ultrasonic measurements have been performed and analyzed for three different rat populations (six controls, four wild hypoxics, and six KO hypoxics). We use a 50 MHz acoustic microscope in double-transmission mode with insonification in the radial direction of the PA wall. Thickness and speed of sound are determined by measuring changes in times-of-flight of ultrasonic signals through a reference path of a nutritive solution and a path substituted with the PA specimen. The slope of attenuation is determined by spectral analysis of these same ultrasonic signals. Current acoustic microscopy results are not yet fully understood. Models from the wild hypoxic rat exhibited an expected increase

in speed of sound (up to 10 %) in the PA trunk compared with that of the controls, which is indicative of stiffening as a result of remodeling due to hypertension (see Figure 3a). However, the speed of sound in the KO hypoxic PAs does not appear to differ significantly from that of the controls. More marked increases (up to 100 %) were observed in slope of attenuation for the PA trunk for both hypoxic models as compared with controls (see Figure 3b). Smaller changes in the ultrasonic properties were observed for either the left or right PA branches. Continuing studies aim to investigate the effect of loading of tissue to mimic *in vivo* arterial pressures and to increase the population counts of the rat models to reduce the large standard deviations.

The histology of the PAs is being evaluated to determine relationships between the structure and properties of the tissue, and to characterize remodeling of structure associated with increases in stiffness measured for patients with PHT. As shown in Figure 4, the extrapulmonary arteries have complex structures

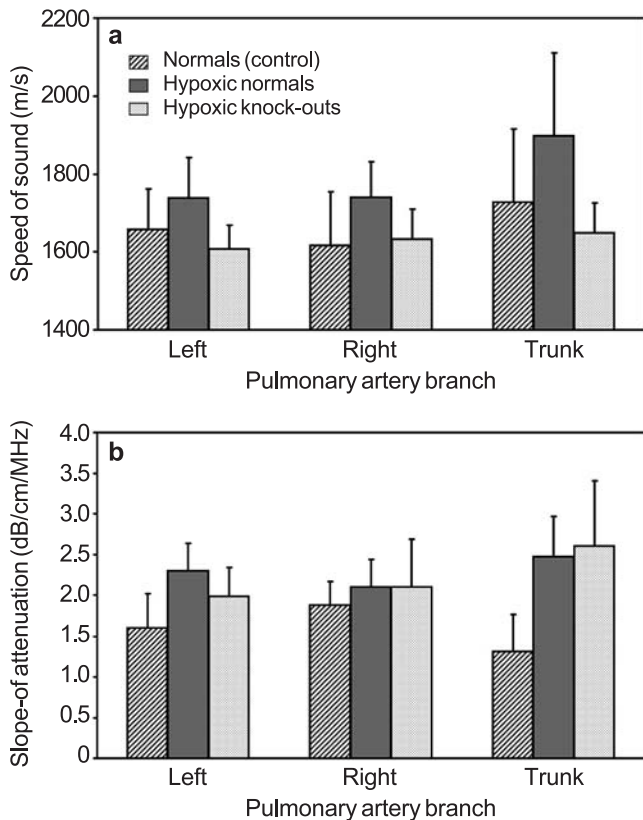


Figure 3: a) Comparison of the speed of sound and b) slope of attenuation in pulmonary branches for controls ($n=6$), hypoxic wilds ($n=4$), and hypoxic KO ($n=6$). Error bars represent standard deviations among the specimens.

that provide the strength and elasticity required for the conduit function and environment.

Current observations indicate that the hypoxic knockouts have collagen deposition and vascularization in the adventitial layer adjacent to the medial layer. In Figure 4, for example, there is a gradient of apparent density through the adventitial layer, where control samples tend to have a structure more like that near the outside diameter of this example. Other measurements, such as elastic lamina thickness, sublayer thickness, and the size of the smooth muscle cells, are also being evaluated.

One of the advantages to conducting this work at NIST is our ability to apply different techniques to the same problem or issue, thereby gaining a more complete understanding of the development

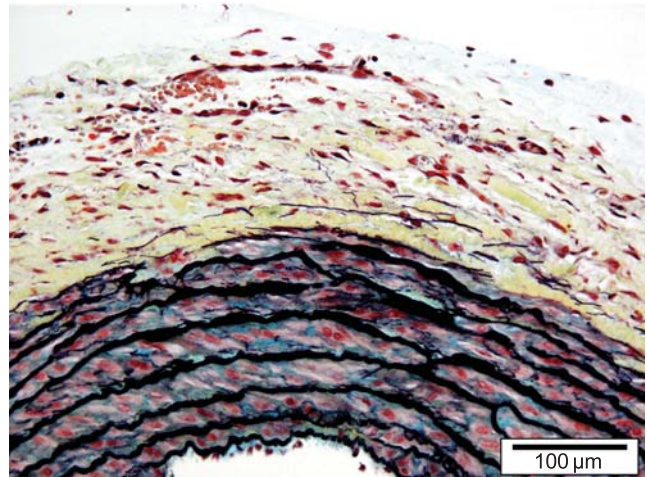


Figure 4: A cross-section of a pulmonary artery, taken just adjacent to the heart in a hypoxic knockout rat, showing the three major layers (endothelial, medial, and adventitial) characteristic of extrapulmonary arteries. The lumen (cavity in which the blood flows) is partially visible at the bottom edge of the figure. The endothelial layer, which is in contact with the blood, is a very thin layer adjacent to the lumen that ends at the first elastic lamella (black bands). The medial layer in this particular artery has about eight elastic lamella that separate it into about seven sublayers of smooth muscle. The adventitial layer is the third layer on the outside diameter of the artery. This layer is typically a fibrous low-density layer compared with the medial layer.

of the pathophysiology of PHT and its effect on the pulmonary arterial mechanics. The elastic properties generated by the acoustic microscope provide the best opportunity for bridging the technical gap between clinical *in vivo* ultrasonic measurements and *in vitro* mechanical properties measured in the laboratory. The complementary work on the histology will help to corroborate the statistical significance in the mechanical properties observed among the populations. Moreover, the histological analysis can contribute to future treatments of PHT directed at the specific cell or biochemical expressions that result in reduced compliance of the arterial wall.

For More Information on this Topic

E.S. Drexler, C.N. McCowan, T.P. Quinn, A.J. Slifka, K.R. Waters (Materials Reliability Division, NIST)

Nanometrology

The burgeoning field of nanomaterials extends across the full range of traditional material classes, including all forms of metals, polymers, and ceramics. No previous materials technology has shown so prodigiously a potential for concurrent advances in research and industry as does the field of nanomaterials in mechanical devices, electronic, magnetic, and optical components, quantum computing, tissue engineering and other biotechnologies, and as-yet unanticipated exploitations of as-yet undiscovered novel properties of nanoscale assemblies of particles. Already, there is growing excitement surrounding the ability of some molecules or particles to self-assemble at the nanoscale to form new materials with unusual properties. Nanometrology, *i.e.*, the ability to conduct measurements at these dimensions, to characterize the materials, and to elucidate the structure and nature of these new and novel assemblies, is a requisite and fundamental cornerstone that must be established securely if this technology is to flourish.

NIST is uniquely positioned to lead the development of the measurement methods, instrumentation, standards, and reference materials that, together, will form the metrological infrastructure essential to the success of nanotechnology.

The MSEL Nanometrology Program incorporates basic measurement metrologies to determine material properties, process monitoring at the nanoscale, nanomanufacturing and fabrication techniques, and structural characterization and analysis techniques such as advanced imaging and multiscale modeling. The Program comprises 22 projects in the Ceramics, Materials Reliability, Metallurgy, and Polymers Divisions, and includes structural characterization using neutron scattering at the NIST Center for Neutron Research (NCNR). The projects cover a wide range of measurement and characterization methods grouped into the areas of mechanical property measurement, chemical and structural characterization and imaging, fabrication and monitoring of nanoprocesses and events, and modeling of nanoscale properties. In each area, we work to advance basic measurement capabilities and lead the intercomparison, standardization, and calibration of test methods. The newly completed Advanced Measurement Laboratory at the NIST Gaithersburg site provides an incomparable environment for accurate nanoscale metrology.

In the area of mechanical property measurement, we are developing and standardizing techniques for determining nanoscale elastic properties (elastic moduli, Poisson's ratio, and internal stress), plastic deformation, density, adhesion, friction, stiction, and tribological behavior. Work in nanoindentation, used extensively

in determining mechanical properties of thin films and nanostructures, focuses on developing traceable calibration methodologies and standard test methods. We also use atomic force acoustic microscopy, surface acoustic wave spectroscopy, and Brillouin light scattering to measure the mechanical properties of thin films. In addition, we are developing micro- and nano-scale structures and test methods to measure strength and fracture behavior of interfaces and materials having very small volumes.

The chemical and structural characterization and imaging utilize neutron and x-ray beam lines at three facilities: the NCNR; the National Synchrotron Light Source at Brookhaven National Laboratory; and the Advanced Photon Source at Argonne National Laboratory. Innovative scattering and spectroscopy methods are advancing our ability to obtain a wide range of chemical and structural information at the nanoscale, including chemical bond identification and orientation, polyelectrolyte dynamics, and equilibrium structures. In collaboration with three other NIST laboratories, we are developing electron microscopy and spectroscopy instrumentation for quantitative, 3D chemical imaging at the nanoscale. Other characterization projects include work on gradient reference specimens for the calibration of advanced scanning probe microscopy, and the application of carbon nanotubes as physical probes of cell membranes.

Efforts in the fabrication and monitoring of nanoscale processes and events include the study of electrochemical and microfluidic methods for fabricating nanostructures, novel approaches to nanocalorimetry for the study of interfacial reactions, *in situ* observations of nanoparticle and nanotube dispersion and alignment, and advanced instrumentation for nanotribology experiments.

Finally, we have extensive efforts in the theory, modeling, and prediction of material properties and behavior extending from nanoscale to macroscale dimensions. Modeling efforts include large-scale finite element methods, multiscale Green's function methods, classical atomistic simulations, first principles, and quantum mechanical calculations using density functional theory. Often, several modeling methods must be combined into one study to accurately describe the material behavior; thus, we pay great attention to the correct interfacing between models operating at different length scales, to ensure that our models properly capture the physics of both components and total systems.

Contact: Stephanie A. Hooker

Metrology for Nanoscale Properties: Brillouin Light Scattering

Brillouin light scattering is being employed to provide information on acoustic and magnetic waves at gigahertz frequencies in thin-film materials. Measurements and modeling in FY04 have focused primarily on interactions of spin waves in ferromagnetic films, elastic constants of nanoporous low- κ dielectrics, and propagation of acoustic waves in nanopatterned polymers.

Ward Johnson, Sudook Kim, and Colm Flannery

Technical Description

Brillouin light scattering (BLS) is an experimental technique that measures the intensity of spectral components of light that is inelastically scattered by vibrational waves (phonons) or spin waves (magnons) in a material. Fabry–Perot interferometric techniques are used to acquire accumulated spectra through repeated mechanical sweeping of the etalon spacing.

BLS is the only laboratory technique that is currently available for detecting magnons of finite wavenumber. Because of this capability and because of innovations in interferometric techniques, BLS has been increasingly applied to problems in magnetics over the past couple of decades.

For characterization of phonons in thin films, BLS offers several advantages over other techniques. Since it detects phonons in the gigahertz range, elastic constants can be determined in films of submicron thickness without the complication of vibrational energy penetrating significantly into the substrate. Modes localized in submicron structures can be characterized. Spatial variations in elastic properties and vibrational patterns can be measured with a lateral resolution equal to the size of the laser focal spot on the specimen (typically, ~ 50 micrometers).

In this division, techniques are being developed for characterizing interactions of magnons in metallic ferromagnetic thin films. Such interactions limit the speed of magnetic-storage devices, spin-valve sensors, and other thin-film magnetic devices.

BLS measurements and modeling of vibrational modes are being pursued in several thin-film systems, including nanoporous low-dielectric-constant (low- κ) dielectrics, nanopatterned polymers, and arrays of molecular rotors.

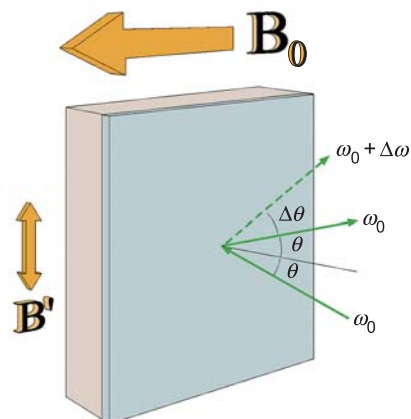


Figure 1: Scattering of light off waves in a thin film.

Accomplishments

During FY04, we developed and applied methods for measuring magnons that arise directly or indirectly from microwave pumping of metallic ferromagnetic films in a static magnetic field (Figure 1). BLS spectra were studied as a function of scattering angle, microwave power, and laser power to provide information on magnon–magnon interactions in $\text{Ni}_{81}\text{Fe}_{19}$. The results demonstrate, for the first time, detection of nonzero-wavevector magnons arising from the decay of pumped uniform-precession magnons in metallic thin films.

Young’s modulus and Poisson’s ratio in nanoporous low- κ dielectric films were measured using conventional backscattering techniques. This research is described elsewhere in this annual report.

Measurements and modeling of vibrational modes in nanoimprinted polymers were pursued in collaboration with the University of Akron and the NIST Polymers Division. In addition to bulk and surface modes, low-frequency modes were detected and found to be consistent with vibrational localization in the imprinted lines. This result suggests the possibility of characterizing elastic properties on a scale of tens of nanometers.

Contributors and Collaborators

P. Kabos (Radio-Frequency Technology Division, NIST); S. Russek (Magnetic Technology Division, NIST); A. Slavin (Oakland Univ.); J. Michl (Univ. of Colorado, Chemistry Dept.); R. Horansky (Univ. of Colorado, Physics Dept.); C. Soles (Polymers Division, NIST); R.H. Hartschuh, A. Kisliuk, and A. Sokolov (Univ. of Akron)

Metrology for Nanoscale Properties: X-ray Methods

Macroscopic properties of technologically interesting materials originate from their underlying micro-structure. To design and understand improved materials, it is necessary to characterize the microstructure and correlate its changes to the macroscopic properties of interest. We especially focus on x-ray diffraction studies of biomedical, ferroelectric, optoelectronic, photovoltaic, semi-conducting, and other materials relevant to the health and microelectronics industries. In particular, studies of microstructural properties, such as strain and stress, crystalline defects, and texture, complement the information obtained by other techniques.

Thomas A. Siewert and Davor Balzar

In this report, we focus on two topics: the studies of superconducting tungsten thin films and comparison of the thin-film texture, as obtained by Electron Back Scatter Diffraction (EBSD) and x-ray diffraction (XRD). Tungsten superconducting transition-edge sensors (TES) are used in different astrophysics and astronomy applications, and as single-photon detectors for the quantum computing experiments. Such detectors comprise thin tungsten films and operate at temperatures close to absolute zero and to the critical superconducting transition temperature (T_c) of tungsten. Thin films, in general, contain both high-temperature α -W phase (with $T_c = 15$ mK) and β -W (A15 cubic structure with $T_c = 1\text{--}4$ K). Close to the T_c , very small thermal changes, such as the absorption of a single photon, increase the film electrical resistance. The result is the production of an electrical output signal that corresponds directly to the detection of the absorbed photon energy. In general, residual stress can influence the T_c of the thin film both directly and by inducing the $\beta \rightarrow \alpha$ phase transformation. Thus, in order to control the T_c , it is necessary to measure and control both the phase composition and residual stresses. Residual stresses in films depend on the preparation conditions, the thickness of the film, and the difference in thermal expansion coefficient between the film and the substrate. The total residual stress results from both the intrinsic (growth) stress and thermal stress. We measured the stress by XRD at both ambient and cryogenic temperatures.

The sample was held in a continuous flow cryostat that was capable of achieving temperatures as low as 8 K. The cryostat was mounted on a goniometer to enable the angle-dispersive XRD measurements. The shift of the α -W {110} Bragg reflection was used to estimate stress at 8 K, and directional measurement

of the {321} lattice spacings ($\sin^2\psi$ method) yielded the total residual stress at ambient temperature. The values obtained are about 0.7 GPa and higher, where the bulk of the stress is due to the intrinsic (growth) component.

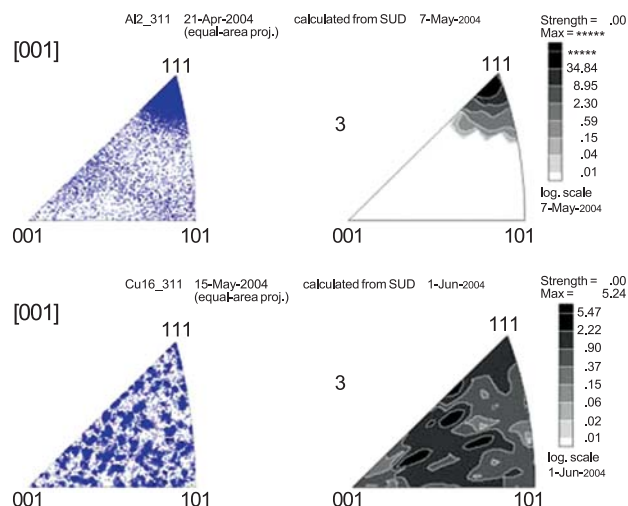


Figure 1: EBSD (left) and XRD (right) inverse pole figures of aluminum (top) and copper (bottom) thin films.

Texture has a large influence on many properties of thin films. XRD was the primary method for the characterization of texture for many years. Recently, alternative local techniques have been developed to bring the measurements to the nanoscale. This year, we compared measurements taken with conventional XRD and EBSD on two thin films: sputtered aluminum and electroplated copper. Both films had a thickness of about $1\ \mu\text{m}$ and were grown on [100] silicon wafers. The inverse pole figures for both samples and techniques are shown in Figure 1. It is obvious that the agreement between XRD and EBSD in case of aluminum film is very good, whereas it is rather poor for copper film. This is a consequence of different penetration depths of electrons and x-rays; while the aluminum sample is homogeneous through the film thickness, copper film is not. After sample preparation, electroplated copper is likely to undergo self-annealing at room temperature. This well-known phenomenon yields a difference in grain size and orientation between the surface and the bulk of the sample.

Contributors and Collaborators

Adriana Lita, Jens Müller, Roy H. Geiss, Dave T. Read, M. Kopycinska-Müller, Robert Keller (NIST); Laura Kaatz, Amitendra Chaudhuri (University of Denver)

Physical Properties of Thin Films and Nanostructures: Grain Size Effects on Actuator Fatigue

Several materials are now produced commercially with particle sizes on the order of 10–100 nm. The availability of ceramic materials in this size classification is particularly important for the electronic component industry. Nanopowders can enable significant decreases in internal layer thickness (for multilayer devices), minimize the size and prevalence of processing defects, and boost the overall performance of components ranging from capacitors to resistive gas sensors. Quantifying these performance enhancements and their dependence on microstructure is a key objective in the Materials Reliability Division.

Stephanie A. Hooker

Many multilayer ceramic devices can benefit from the use of ultra-fine powders, including passive electronic components, gas sensors, and miniature actuators. However, fabrication issues associated with processing these high-surface-area powders have hindered their commercialization. Key challenges have included nanopowder reproducibility, optimization of processing slurries, and control of sintering profiles to produce the desired micro/nanostructure characteristics. Moreover, in many cases, predicting the optimum microstructure features for maximum performance is quite difficult, and extensive experimentation remains necessary.

One specific component that can benefit from the use of nanopowders is the multilayer piezoelectric actuator. These devices generate precise, controlled motion for translating optics, damping vibrations, redirecting air flow, and dispensing fluids. Each component consists of many active layers, the thickness of which determines the device's power requirements. Layer thickness is typically on the order of several hundred microns for conventional actuators and is driven by the need for many individual piezoelectric grains to span the active layer, thereby reducing the chance for electrical failure. Reducing grain sizes from micrometer to submicrometer scales enables dramatic decreases in layer thickness, reducing power needs and increasing applicability.

However, at issue is the piezoelectric response and, in particular, the long-term fatigue resistance. Fatigue is the change in polarization or displacement over time and is a recognized problem for state-of-the-art actuators. Because processing-induced defects tend to be on the scale of the starting powder, nanopowders can improve mechanical durability. However, a corresponding

decrease in ferroelectric response is also anticipated as grain size reduces. Fatigue is affected by both the mechanical and electrical responses, making its prediction quite difficult for fine-grained components.

In FY04, we investigated the fatigue behavior of 14 microstructures obtained by controlled sintering of 80-nm PZT-5A powders. The devices tested were 1206-sized (0.30 cm × 0.15 cm, or 0.12" × 0.06") chips, each with 10 active layers (50 μm thick). Characterization included dielectric, impedance, and ferroelectric properties, as well as short- (<1 million cycles) and long-term (1–100 million cycles) degradation under combined electrical and mechanical influences.

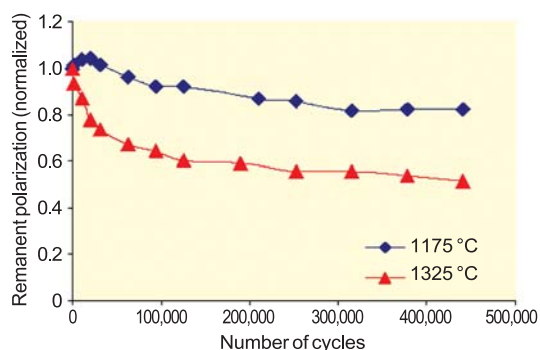


Figure 1: Effect of sintering temperature on ferroelectric fatigue.

The results clearly demonstrate the dependence of fatigue on microstructure. Figure 1 compares changes in remanent (*i.e.*, permanent) polarization over time when devices were cycled using a 35 Hz sinusoidal wave with an amplitude of ± 75 V. The average decrease in polarization for the finest-grained materials (sintered at 1175 °C) was less than 20 % after 0.5 million cycles, compared to nearly 50 % for larger-grained components.

In FY05, we will expand on this work and examine the corresponding effects on displacement and domain reorientation for devices with even thinner internal layers. The resulting data will then be used to validate the suitability of these components for biomedical and smart structures applications, both of which demand high performance and long operational lifetimes.

Contributors and Collaborators

R. Geiss (Materials Reliability Division, NIST);
C. Kostecky, D. Deininger, K. Womer (Synkera Technologies)

Physical Properties of Thin Films and Nanostructures: Nanoporous Low- κ Dielectric Films

Nanoporous low-dielectric-constant (low- κ) films present considerable implementation challenges for the microelectronics industry and also raise new scientific questions. We apply optical methods to these films to evaluate such critical properties as density/porosity, Young's modulus, and Poisson's ratio. Our techniques allow measurement of properties that are otherwise difficult to determine and shed light on how the mechanical properties depend on porosity.

Colm Flannery and Donna C. Hurley

Current miniaturization trends in microelectronics require faster device switching. This need can be at least partially met by lowering the resistance-capacitance factor of the dielectric materials. One promising solution is to introduce nanometer-sized pores that reduce the dielectric constant κ . Unfortunately, introduction of porosity may lead to a drastic reduction in stiffness (Young's modulus), adversely affecting the material's chances of surviving the fabrication process. In addition to predicting and ensuring process reliability, accurate values of a film's mechanical properties are needed to model the mechanical behavior of the resulting microelectronics device. New tools are needed to characterize these relevant thin-film properties (e.g., Young's modulus and Poisson's ratio ν), as well as to better define their dependence on porosity.

In FY04, we evaluated Poisson's ratio ν in methylsilsequioxane (MSSQ) polymer films of varying porosity with Brillouin light scattering. In this technique, a Fabry-Perot interferometer detects frequency-shifted photons scattered by ambient thermal phonons in the material. The frequency shift of the photons is characteristic of the acoustic phonon modes in the film. Values of ν were determined from measurements of both longitudinal and surface acoustic wave modes. Figure 1 reveals that ν decreases as porosity increases. The results

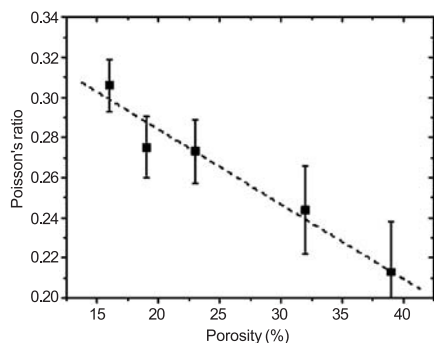


Figure 1: Measured Poisson's ratio vs. porosity for MSSQ films.

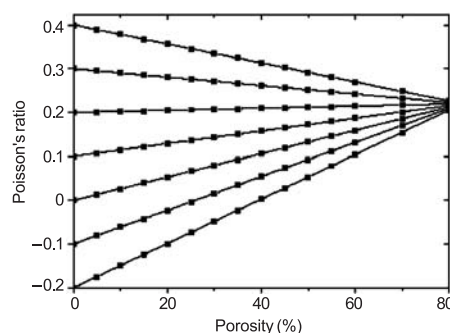


Figure 2: Predicted dependence of Poisson's ratio on porosity.

of an existing finite-element model, shown in Figure 2, predict that ν will either decrease or increase depending on the initial ν of the matrix material. In addition, ν tends towards a constant value of 0.2 for all materials at high porosity. Our measurements are consistent with the model. However, they show a much larger rate of decrease in ν , probably because a percolation threshold had been reached. Quantitative results like these will prove valuable for modeling of structures involving low- κ films. The results also yield insight into the porosity dependence of ν , about which very little is known.

A second method to determine thin-film properties involves the frequency-dependent dispersion of laser-generated surface acoustic waves (SAWs). In FY04, efforts concentrated mainly on the development of a standard SAW data analysis procedure. With careful signal processing that minimizes sensitivity to noise and maximizes the frequency range of the measured signals, we can extend the frequency range of our measurements by 20%. The result is a significant reduction in the uncertainty of the extracted film properties. The method lends itself to automation and has allowed us to inspect films less than 300 nm thick. (Previously, films less than 500 nm thick were challenging.)

The improved measurement procedure, combined with new multilayer Green's function analysis software, has allowed us to inspect multilayer structures. With these capabilities, we have extracted properties of thin (50–100 nm) capping layers of stiffer materials on top of more compliant functional films. In addition, the Young's modulus, density, and thickness of the underlying dielectric films were evaluated.

Contributors and Collaborators

S. Kim, V. Tewary (Materials Reliability Division, NIST); Y. Liu (International Sematech); J. Wetzel (Tokyo Electron America)

Physical Properties of Thin Films and Nanostructures: Green's-Function Methods

Precise knowledge of atomistic configuration and strains in nanomaterials is needed for their characterization and development of new devices. We have developed computationally efficient Green's-function methods for calculation of lattice distortion, elastic strains and displacements in a variety of material systems. Our work is useful for interpretation of data obtained by AFAM, nanoindentation, and SAW experiments.

Vinod K. Tewary and Bo Yang

Technical Description

Green's function (GF) provides a computationally efficient tool for interpretation of data obtained by nanoindentation and atomic force acoustic microscopy (AFAM) which is useful for elastic characterization of nanomaterials. The dynamic GF is used for modeling propagation of surface acoustic waves (SAWs) in solids and their phonon properties. The GF accounts for interfaces and free surfaces in the solid and its elastic anisotropy, which play relatively important roles in the elastic response of nanomaterials as compared to ordinary solids. We use GF to calculate the elastic displacement fields, interaction energy between the embedded nanostructure and other defects and free surfaces. The displacement field, due to a force at the surface, is used for interpretation of AFAM and nanoindentation measurements. The interaction energy of the nanostructures is an important factor in the stability and growth of the nanostructure.

We have developed GF methods both at the discrete atomistic and macro continuum scales. For a lattice model containing N atoms, the GF is given by:

$$\mathbf{G} = \mathbf{\Phi}^{-1}$$

where \mathbf{G} and $\mathbf{\Phi}$ are $3N \times 3N$ matrices of GF and force constants respectively. The matrix inversion is carried out by using the discrete Fourier transform for a perfect lattice or numerically by computer simulation for a model crystallite as in molecular dynamics.

In order to model an embedded nanostructure in a host solid, or a thin film on a substrate, we define an initial GF for the host and the final GF. The final GF is related to the initial GF through the Dyson equation.

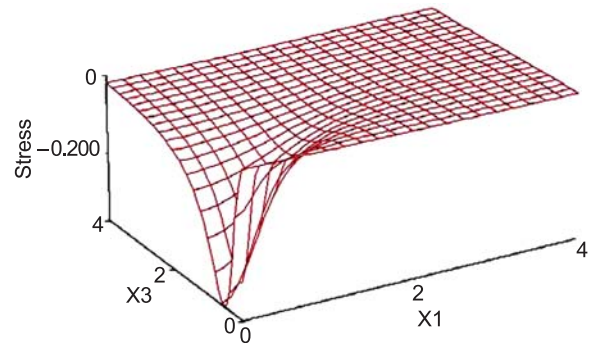


Figure 1: Stress distribution in Si due to a surface load.

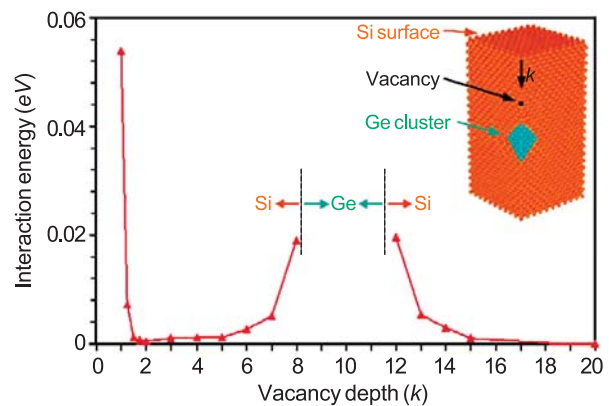


Figure 2: Interaction energy of a cluster of 147 Ge atoms with a vacancy and free surface in Si.

In the continuum model, we simulate free surfaces and interfaces by applying the usual boundary conditions.

Accomplishments

We have carried out a detailed analysis of SAW measurements in a thin TiN film on Si, calculated stresses in a wide range of solids, and modeled Ge clusters in Si containing a free surface and a vacancy. The work is reported in six papers. A library of GFs is available at www.ctcms.nist.gov/gf, which contains downloadable teaching and tutorial material on GFs and computer codes for calculation of GFs. A GF group of about 50 international users has been formed at CTCMS.

Contributors and Collaborators

D. Hurley, D.T. Read (Materials Reliability Division, NIST); L. Bartololo (Kent State University); A. Powell (M.I.T.)

Applications of Carbon Nanotubes: Carbon Nanotubes and Nanotube Contacts

A critical requirement for developing carbon nanotube based electronics is determining the mechanical and electrical characteristics of the connection between the carbon nanotube and its electrode. On this scale (nanometers), the properties of both the nanotube and the contact are not scaleable from larger measurements. To address this issue we are exploring a technique commonly used to manipulate the nanotubes and attach them to substrates inside the scanning electron microscope. We are subsequently developing the techniques to measure the small electrical currents and test the small mechanical strength associated with the contacts and nanotubes.

Paul Rice

We are developing techniques to measure the mechanical and electrical properties of carbon nanotube-based devices and also to image the nanometer-scale structure within the nanotube and their electrical contact. Shown in Figure 1 is a test device that we have fabricated to measure the electrical characteristics of an individual multiwalled carbon nanotube. The nanotube was attached, or welded, to the device in the scanning electron microscope (SEM) using an accepted technique called electron beam deposition (EBD). In this example, a single tube extends from one electrode to another.

Understanding the mechanical properties of the weld requires visualizing its structure on the atomic scale if

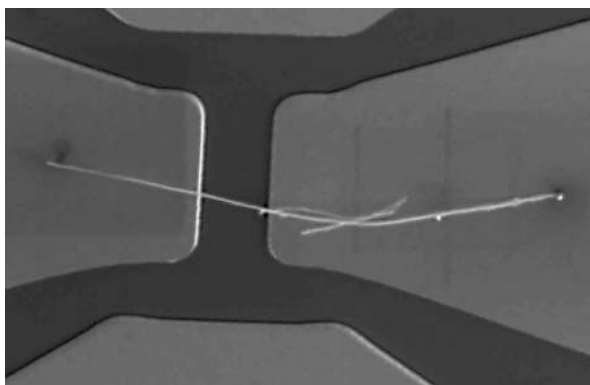


Figure 1: SEM image of carbon nanotube test device for electrical measurements. The nanotube extends across a 2 μm gap. A second accidental tube is hanging on the side and is not connected to the electrodes.

possible. Using high-resolution microscopy techniques available within the division, we have seen some interesting new structures of the weld. Previously, it was assumed that the weld was a uniform material composed of amorphous carbon. However, we have seen, using atomic force microscopy (AFM) as well as transmission electron microscopy (TEM), spurious deposits of carbon far outside the weld. Figure 2 shows a nanotube welded to a chromium film. The residual carbon is seen as a surface texture that covers almost everything including the nanotube.

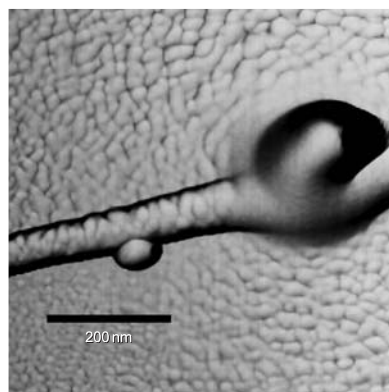


Figure 2: AFM image of a multiwalled carbon nanotube welded to a chromium film. The orange peel texture is residual carbon left behind from the weld process.

This work is beginning to shed some light on the properties and structure of these very small devices. A paper has been submitted entitled, "Electron Beam Deposition Welding: A Practical Application to Building Carbon Nanotube Devices," by P. Rice, R.H. Geiss, S.E. Russek, A. Hartman and D. Finch, to the *Journal of Vacuum Science and Technology B*. Further work is planned to measure contact resistance within the weld and resistance changes due to distortions caused by the weld process.

Demonstrating the need for better standards for nanotube device characterization, a new standards committee was recently formed by IEEE, on which NIST currently serves as a contributing member. Furthermore, presentations have been given to the American Vacuum Society, NASA Johnson Space Center, and the engineering department of the University of Colorado.

Contributors and Collaborators

R. Geiss (Materials Reliability Division, NIST); S.E. Russek, P. Kabos (EEEL, NIST); D. Finch, A.B. Hartman (University of Colorado)

Applications of Carbon Nanotubes: Cell Viability in Contact with Carbon Nanotubes

With the recent excitement about carbon nanotubes and their biological applications, preliminary studies are underway to determine the biocompatibility of nanotubes with cell cultures using our vascular smooth-muscle cell line. The response of these cells will help us understand the effects of cell proliferation or degradation due to direct contact with nanotube mats or clusters.

Paul Rice and Tammy Oreskovic

Carbon nanotubes (CNTs) have great potential for nanometer scale electronics, superior strength composites, biological implants, and many other applications where a well-organized nanometer scale material is needed. One possible application is using nanotubes as scaffold materials to support the growth of transplanted cells and establish proper orientation to grow artificial tissue. NASA has recently demonstrated growing retinal cells on nanotube mats. Other possible applications include sensors and probes for miniature biological devices, and electrodes for detecting biomolecules in solutions. However, many issues still remain in assessing the biocompatibility of these nanomaterial biosystems for *in vivo* applications.

In FY04, we explored the viability and proliferation of cells in contact with carbon nanotubes and

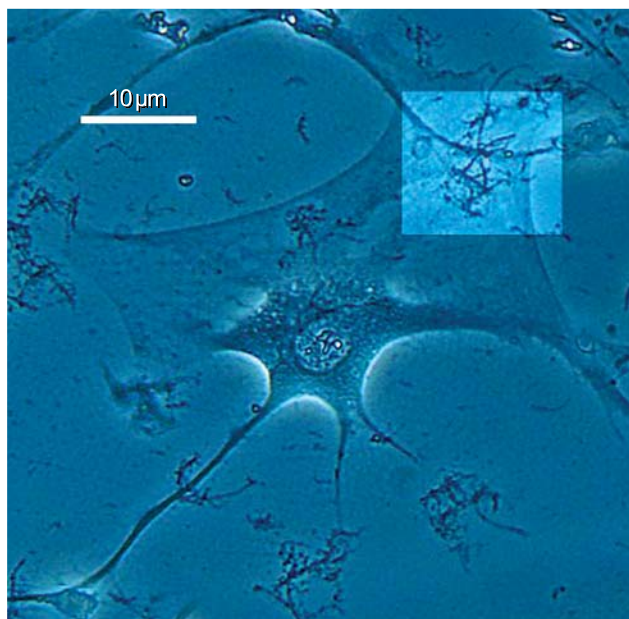


Figure 1: Vascular smooth muscle cell growing on a cluster of multiwalled carbon nanotubes on a glass substrate.

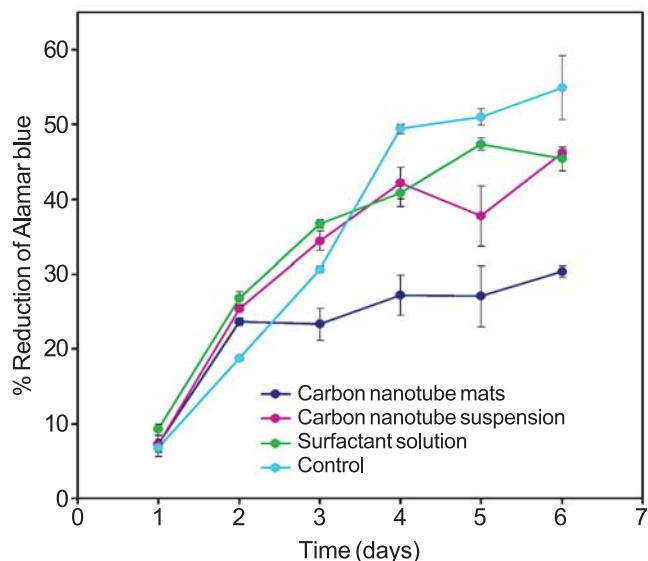


Figure 2: Alamar blue assay, test for cell growth and proliferation. As the cells grow and divide they metabolize the Alamar blue compound, changing the medium in which the cells are growing from a blue color to clear.

dispersion techniques for compatible surfactants in cellular environments. In preliminary experiments, smooth muscle cells were exposed to both entangled mats and suspensions of multi-walled CNTs by use of surfactants for dispersion (Figure 1). Results of the proliferation assay indicate that there is a reduction in growth and metabolic activity for cells grown directly on the nanotubes as compared to the controls. These results indicate that cell attachment may not be as strong in regions of high CNT density. However, if the nanotubes are coated with a biologically compatible surfactant and suspended in media, there appears to be little effect when compared to the controls. Figure 2 shows preliminary results of an Alamar blue proliferation assay.

In FY05, we will continue to explore the interactions of structure and the effects of clumping of CNTs on cell growth and orientation. Other possible directions may include surface modification to promote cell adhesion and growth, tomography, and size distribution of CNTs.

Contributors and Collaborators

Dr. N. Varaksa contributed the work on the surfactant chemistry; Dr. E. Gruelky (University of Kentucky) supplied carbon nanotubes.

Applications of Carbon Nanotubes: Electrochemical Characterization of *In-Vivo* Neuronal Probes

Instruments for *in-vivo* recording of neural activity are critical for ongoing and future research aimed at Alzheimer's, Parkinson's, epilepsy, stroke, and spinal cord injuries. In addition, the development of a human-brain-machine interface (HBMI) relies on improved recording and processing of neuronal signals. Future recording electrodes must be small, stable, biocompatible, and robust. More rugged test procedures are also needed for evaluating and qualifying new electrode materials.

Stephanie A. Hooker and Dudley Finch

New tools are needed to better image and measure signal transfer inside live cells. One conventional approach to electrical measurements in cellular materials involves a two-electrode glass micropipette that clamps the cell membrane. The discovery of this device, referred to as a patch clamp, in 1972 had widespread impact, leading to a Nobel Prize in 1991. However, the patch clamp is too large for many of today's desired measurements in neurobiology, due to the extent of physical damage caused during its insertion and use.

Recently, silicon-based MEMS technology has been explored as a method to produce smaller probes for neuronal research. These devices typically consist of a silicon shank (several hundred micrometers long) with an array of microelectrode recording sites located along its surface. In this manner, multiple neurons can be studied simultaneously with a single insertion point.

While these devices show considerable promise, many biologists continue to employ individual metallic wires as their primary recording electrodes. These wires are similar to those used inside the patch clamps but are inserted directly into the brain. Polymer coatings are often applied to increase impedance, enable better handling, and improve biocompatibility. The wires are typically tungsten or stainless steel with diameters on the order of 50–100 microns. To date, few studies have attempted to optimize the wire material, the coating, or the insertion technique (applied force, speed, etc.).

In collaboration with the University of Colorado's Health Sciences Center and the Departments of Chemistry, Electrical Engineering, and Mechanical Engineering at the University of Colorado at Boulder, we are developing measurements to help improve and optimize *in-vivo* probes. In FY04, we completed preliminary studies of wires (25 μm in diameter) coated with thin (~ 60 nm) layers of aluminum oxide, Al_2O_3 . Atomic layer deposition (ALD) was used to precisely

control coating thickness, and seven different wires were compared to determine metal effects on performance.

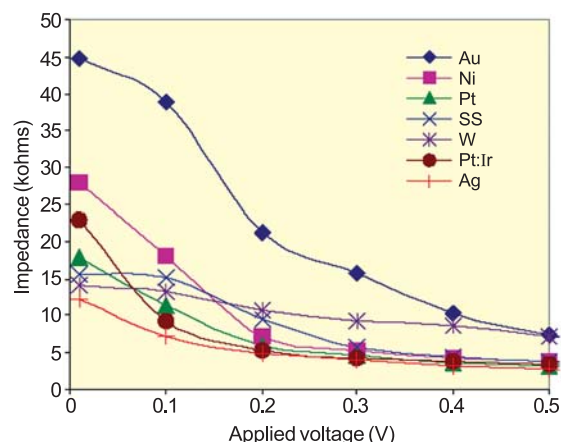


Figure 1: Electrochemical impedance of ALD-coated microwires in Ringer's solution as a function of applied voltage at 100 Hz.

A two-electrode configuration was used for testing in a Ringer's buffer solution. Several procedural variables were evaluated, including the type and size of the reference wire, the solution temperature and pH, and the electrode placement. Impedance was measured as a function of frequency, voltage (Figure 1), and time. The latter indicates the stability and reliability during extended recordings, a key requirement for long-term studies. Stability measurements will continue during the upcoming months in order to ensure that the ALD coating is not degraded either chemically (by the solution) or electrically (by the measurement itself).

However, it should be noted that 25 μm wires are still too large for subcellular studies. As a result, we plan to evaluate carbon nanotube (CNT) probes in FY05. CNT-based AFM probes have already been developed by other researchers in the Materials Reliability Division for studying microelectronic films. Moreover, dielectric coatings have recently been applied to individual tubes (via ALD) to further enhance signal transfer. If successful electrochemical measurements can be demonstrated, CNT based *in-vivo* probes could have a significant impact on neuroscience due to their small size (0.1 μm or less) and anticipated long-term stability.

Contributors and Collaborators

D. Restrepo, A. Sharp (University of Colorado Health Sciences Center); R. Artale, K. Gall, S. George, R. Zane (University of Colorado at Boulder)

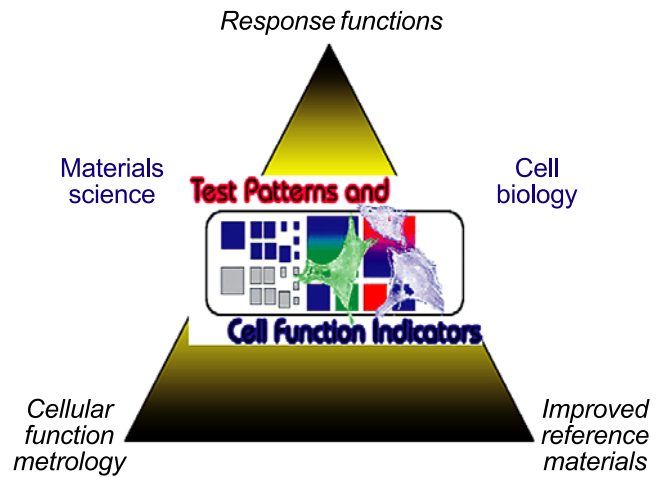
Biomaterials

New materials and devices are radically changing the treatment of injury and disease, yet it is clear that within this rapidly evolving segment of the materials industry, a basic measurement infrastructure does not exist. The Biomaterials Program develops measurement methods, standards, and fundamental scientific understanding at the interface between the materials and biological sciences. For the health care industry, we focus on dental and medical sectors that apply synthetic materials for replacement, restoration, and regeneration of damaged or diseased tissue. Three primary foci exist within this program: biocompatibility, biomaterials characterization, and materials measurements applied to biological systems.

Whether the medical issue involves implanting a hip- or knee-joint prosthesis, a synthetic bone graft, or a tissue engineering scaffold into the human body, one primary issue is biocompatibility. Using our expertise in materials science, we have developed suitable Reference Materials (RM) for investigating biocompatibility and implant suitability. Research has focused on measuring cellular response to powders and bulk materials that are candidates for implants; recently, we produced a realistic wear particle Standard Reference Material (SRM[®] 2880) for bioactivity testing.

Work on quantitative methods of biomaterials characterization includes assays for adhesion, viability, proliferation, and differentiation of bone cells, 3-dimensional structural/functional imaging of tissue in-growth, and biochemical assays to quantify inflammatory responses to synthetic materials. The focus of this effort is bridging the gap between fundamental knowledge and the product development needs in industry. For example, in collaboration with the Chemical Science and Technology Laboratory, we are developing measurement methodologies and reference materials to assess interactions in complex systems of living cells with synthetic materials. The expected outcome of this work includes reference substrates that induce specific cellular responses, and engineered DNA vectors to act as fluorescent reporters of cellular responses.

Another example of our effort to bridge this gap is our collaboration with the dental industry, which is primarily composed of small manufacturers with limited R&D capability. Collaborations with the American Dental Association Foundation (ADAF) develop improved materials and materials measurements techniques, patent and license these inventions, and, most importantly, provide a technical foundation. Research focuses on improved understanding of the synergistic interaction of the phases of polymer-based composites and the mechanisms of adhesion to dentin



and enamel. This approach will ultimately lead to materials with improved durability, toughness, and adhesion to contiguous tooth structure. We also collaborate with the ADAF to develop metrology for the biocompatibility of synthetic bone grafts.

In this era of interdisciplinary research, we provide an added dimension. By taking a physical/mechanical approach to how cells function, respond, and remodel in interaction with synthetic materials, we provide skill sets typically absent in the biomedical community. Mechanical properties issues also arise when considering synthetic bone grafts and tissue engineering scaffolds. Complementing traditional bulk mechanical property measurements, combinatorial approaches are being developed to identify compositions and surface features that affect properties such as biocompatibility and mechanical durability.

Our mechanical property metrology extends further to biological systems that span the range from individual neurons and muscle cells to complete pulmonary arteries. This necessitates the development of unique mechanical testing platforms and application of a materials science approach to understanding integrated properties. Recently, we have developed a bioreactor capable of applying biaxial stresses and allowing monitoring of the stress and strain of a two-dimensional scaffold sheet during tissue growth.

Fundamental to the Biomaterials program is recognition of the need for an integrated systems approach. Collaborations among and between project teams are critical to progress against the ambitious goals of this program.

Contact: Elizabeth S. Drexler

Biomaterials Metrology: Pediatric Pulmonary Hypertension

Pulmonary hypertension is a potentially fatal complication of congenital heart defects in children who live at high altitudes. Discovering the pathophysiology and expression of the disease may open the way to finding new, more effective diagnostics and treatments. Our contribution to this goal is to provide data on the mechanical properties of the pulmonary artery and its constituents in healthy and diseased tissue.

Elizabeth S. Drexler

Background

Children born with heart defects (~ 1.0 %) have an increased risk of developing pulmonary hypertension at the high altitudes of the Rocky Mountain region. The mechanisms for developing this potentially fatal complication are not clearly understood. It is known that the heart becomes enlarged while trying to maintain a constant flow volume. A cyclic response whereby the heart increases pressure to maintain flow volume and the pulmonary arteries (PAs) remodel to compensate for the increased stress on the walls will ultimately result in morbidity or mortality if not treated.

Technical Strategy

The goal of the project is to determine the critical factors in the development of pulmonary hypertension in children so that we can prevent or mitigate the effects. The strategy is to characterize the fluid dynamics of the system, and identify how, where, why, and over what period the tissue of the artery remodels. The “how” will be answered through measurement of the mechanical properties; the “where” through the histology of the artery; the “why” through study of the biochemical signals that cause the tissue to remodel; and the time frame by using input from all the preceding. Our contribution will be to measure and compare the mechanical properties and histology of PAs using animal models. Our collaborators will perform the clinical and biochemical studies. Tests are conducted within 24 hours of excising the arteries, so that the cells are still viable and responsive. A bubble test is used to obtain stress–strain data, and an acoustic microscope is used to obtain speed of sound and attenuation from the PAs of control, monocrotaline-treated, and hypoxic rats. An additional population of hypoxic rats (knockouts) that are missing the endothelin B receptor (responsible for the expression of vasodilators) has been tested.

Accomplishments

Data from the PAs of 10 monocrotaline-treated rats were reduced and analyzed in FY04. Additionally, the PAs from 12 hypoxic knock-out rats, six hypoxic normal rats, and 12 control rats were tested and analyzed. Figure 1 shows the data from six rats each for the control and hypoxic knockout conditions. It is clear that the PAs from hypoxic rats demonstrated less strain at a given stress than did the controls. The PAs from the monocrotaline-treated rats did not display overtly different stress–strain behavior as compared with the controls.

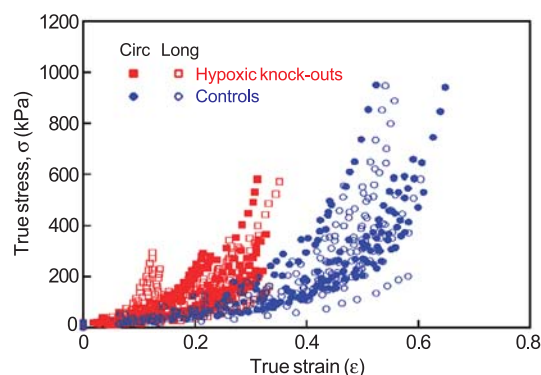


Figure 1: Comparison of hypoxic and control data from the proximal arteries of rats.

We believe that monocrotaline may not be an effective agent for inducing hypertension in the extrapulmonary arteries. The PAs from the hypoxic normal rats also exhibited stiffer behavior than did the controls, but not to the extent of the knock-out hypoxics. The histology indicates that the adventitial layer is thicker in the hypoxic PAs due to collagen deposition, but no obvious differences were observed between the PAs of the controls and the monocrotaline-treated rats. Fixturing has been developed and preliminary results from the acoustic microscope have been generated and are being analyzed. Studies continue to determine the differences in the remodeling of the arterial walls and how those disparities influence the mechanical properties. Analysis of the data in light of general material thickening is being pursued.

Contributors and Collaborators

Chris McCowan, Tim Quinn, Andy Slifka, Kendall Waters, Joyce Wright (Materials Reliability Division, MSEL, NIST), D. Vecchia, J. Splett (Statistical Engineering Division, ITL, NIST); R. Shandas (University of Colorado); K. Colvin, D. Ivy (University of Colorado Health Sciences Center and Children’s Hospital of Denver)

Biomaterials Metrology: Mechanical Response of Tissue Engineering Constructs

Tissue engineering offers the hope that diseased or injured structures within the body can be replaced by tissues grown on scaffolds. To be effective, test methods for the mechanical properties of the polymeric scaffold with and without tissue ingrowth must be developed and the properties themselves measured.

Timothy P. Quinn and Tammy L. Oreskovic

Background

A proposed method for treating disease and injury in the human body is to replace the diseased tissue with tissue that is grown outside the body. Typically, healthy tissue is cultured to grow into a synthetic or natural scaffold. The scaffold supports the tissue and coaxes it to grow into the proper geometrical shape. The scaffold can be cultured with cells *in vitro*, or a bare (or initially seeded) scaffold can be used. In both cases, the mechanical properties of the scaffold or scaffold/tissue construct must be known in order to ensure that it does not fail mechanically after it is implanted. A typical approach would be for the implant designer to use a finite element model to predict the response of the implant to *in vivo* loads. The mechanical quality of the scaffolds must be assured before they are implanted as well.

Mechanical Models

In collaboration with the Polymers Division, an unseeded poly(ϵ -caprolactone) (PCL) scaffold was mechanically tested in compression, and the resulting stress–strain curves were fitted with empirical models. The pore structure of the scaffold was varied by changing the randomly distributed pore size. The models are hyperbolic in form: $\sigma = E \frac{\epsilon}{1 + A\epsilon}$. The hyperbolic model was compared to the secant modulus used for rigid cellular plastics as recommended by ASTM (Table 1).

Table 1. Summary of results of model parameters and pore size

Pore Size Area (mm ²)	E (MPa)	A	Secant Modulus (MPa)
0.0014	89 ± 40	19 ± 10	30 ± 5*
0.0039	122 ± 60	21 ± 13	38 ± 6
0.0150	144 ± 58	31 ± 18	36 ± 5

* Significantly different ($p < 0.05$) from the secant modulus of the other two pore size samples. No other parameters showed significance.

Optical coherence microscopy (OCM) was used to scan the interior of the scaffold samples, and the pores were measured automatically with image analysis software. The OCM images were also used to form the basis of finite element (FE) models that were used to predict the initial elastic modulus of the scaffold (E). Each 4 μm pixel of the OCM image was represented with a brick element and assigned the Young's modulus of bulk PCL, and a value of 0 for a pore. A compressive strain was imposed on the model, and the resulting stresses were calculated. The elastic constants of scaffold were then calculated by use of Hooke's law for a linear-elastic, isotropic material.

The stress–strain curve of the porous PCL cannot easily be approximated with a line up to 10 % strain. However, the hyperbolic model has the drawback of having relatively large standard deviations in its fitted parameters E and A but is the best fit for the non-linear stress–strain curve. The secant modulus offers a much lower variability and could be used for quality control. The results from the FE model are within one standard deviation of the experimental values of E (the initial modulus).

Novel Bioreactors



Figure 1: The copper-colored load cells measure the applied force in this biaxial bioreactor. The sample is held in the center of the fixture and can be imaged from below to measure strain. The sample is bathed in nutrients (not shown), and the nutrient is also pumped across the surface of the scaffold through the grips.

A bioreactor capable of applying biaxial stresses (Figure 1) has been developed. The applied stress and strain of the two-dimensional scaffold sheet can be monitored while the tissue is growing.

Contributors and Collaborators

J.D. McColskey, C.N. McCowan (Materials Reliability Division, NIST), F.A. Landis, N.R. Washburn (Polymers Division, NIST)

Biomaterials Metrology: Cellular Level Measurements

Techniques and tools that facilitate the exposure of single cells (and arrays) to control and quantify mechanical forces, and at the same time allow for the characterization of other biological phenomena, are needed for the study of cardiovascular tissues and cells. The development and evaluation of one of these tools, an optical tweezer, is a focus of this year's effort.

Christopher N. McCowan and Andrew J. Slifka

Overall, the challenge is to develop mechanical test platforms and tools that can be integrated with currently used biological techniques for the evaluation and measurement of cellular response (e.g., gene expression, cell morphology, area of adhesion, etc.). These types of studies are needed because the development of vascular smooth muscle cells in cardiovascular tissue, for example, depends on the variations in the stress-strain environment that result from the expansion and contraction of the vessel wall. The importance of the environment becomes apparent when one considers that engineered tissues have mechanical properties inferior to those of naturally grown tissues. This is possibly a bulk effect, but is clearly related to processes at the cellular level. Without a quantitative understanding of the mechanics and functionality of the building blocks (cells and fibers), the bulk properties of the tissues cannot be fully understood and modeled.

The focus for this year was to build an optical trapping system, including a force/displacement measurement loop. This system will be used to calibrate MEMS devices designed for testing single cells, in addition to measuring cellular components. To facilitate this effort, we are collaborating with David Marr at CSM, who has two optical tweezers. A fluid-flow channel for the calibration of the tweezers has been built. This flow channel will allow us to calibrate the tweezers using a drag force, or Stokes method, and will be compared with methods of calibration based on Brownian motion.

We have calibrated Bio-MEMS devices using the atomic force microscope (AFM). Figure 1 shows one of the devices and a 180 μm long AFM cantilever used for force calibration. The central platform of such a

device would hold a cell that would then be subjected to a controlled, oscillating mechanical environment. This device operates in a suitable fluidic environment that keeps the cell viable and allows for biological assay measurements.

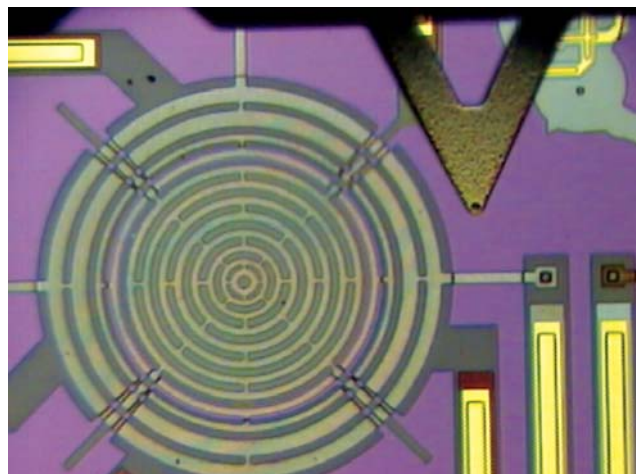


Figure 1: A Bio-MEMS device used to apply controlled forces to cells.

Our first application of the tools developed in this program will be to measure mechanical properties of leukocytes. This will be done in collaboration with Dr. Worthen of National Jewish Medical and Research Center, who has been studying the role of polymorphonuclear leukocytes, or neutrophils, in acute lung inflammation. The neutrophil is larger than the capillaries in the vascular bed of the lung. Therefore, details of the deformation of the neutrophil and capillaries are important in determining the mechanisms of pulmonary inflammatory response. We plan to develop tools such as optical tweezers and MEMS devices to apply and sense deforming forces on cells such as neutrophils.

Contributors and Collaborators

D.S. Finch, T. Oreskovic, D. Lauria (Materials Reliability Division, NIST); R. Rorrer (Mechanical Engineering, CU Denver); D. Marr, J. Oakey (Chemical Engineering, Colorado School of Mines); D. Serrell, H. Panchawagh (Mechanical Engineering, CU Boulder)

Biomaterials Metrology: Quantitative Ultrasonic Characterization

Quantitative ultrasonic characterization of biological materials is the application of physical acoustics techniques to biological and medical problems. The mechanical vibrations of ultrasound involve frequencies from below 1 MHz to over 100 MHz with corresponding length scales from millimeters down to tens of micrometers. Quantitative measurement of propagation and scattering properties enables evaluation of the health and quality of biological materials.

Kendall R. Waters

Background

The biological and medical research communities are often interested in the health or quality of a biological material. Measurement of the mechanical properties of the material can provide information complementary to that determined from biochemical measurements. Furthermore, longitudinal studies monitor materials over an extended length of time, often requiring measurements to be performed nondestructively. Ultrasonic measurement techniques permit nondestructive evaluation of the mechanical properties of biological materials.

Materials can be characterized by their ultrasonic propagation and scattering properties such as phase velocity and attenuation coefficient. In quantitative ultrasonic characterization of biological materials, changes in ultrasonic properties can be correlated to changes in structure and morphology, which then can offer insight into a disease process, for example.

Technical Strategy

We are interested in several classes of biological materials, including soft and hard tissues and engineered biomaterial constructs. Ultrasonic measurements of pulmonary arteries (PAs) from rat models are performed to understand the mechanical effects of pulmonary hypertension. A collaboration with Dr. B. Hoffmeister investigates how ultrasonic properties of cancellous bone depend on bone mineral density, a key factor in the risk of fracture in osteoporotic patients. Another collaboration, with Dr. K. Anseth, investigates the propagation and scattering properties of a tissue-engineered construct of bovine cartilage and hydrogel seeded with chondrocytes (cartilage cells).

For the majority of measurements, we use an acoustic microscope in double-transmission and

backscatter modes to determine propagation and scattering properties. Thickness and speed of sound are determined by measuring changes in times-of-flight of ultrasonic signals through a reference path and a path substituted with the biological material. Attenuation is determined by spectral analysis of the same ultrasonic signals.

Accomplishments

Measurements of PAs from three different rat models (controls, hypoxics, and knock-out hypoxics) have been performed. See the Technical Highlight on Pediatric Pulmonary Hypertension for a summary of results.

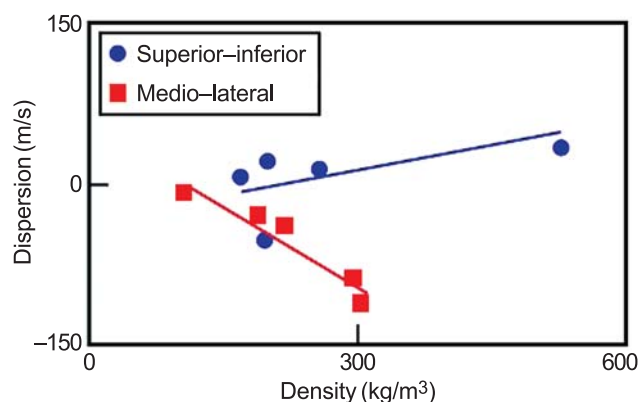


Figure 1: Relation between dispersion and density for bovine cancellous bone in superior–inferior and medio–lateral directions.

Phase-spectroscopic analysis of measurements in the medio–lateral (ML) and superior–inferior directions of ten cancellous bone specimens (bovine tibia) has been completed. Dispersion (frequency dependence of phase velocity) correlated well with density for ML specimens, as shown in Figure 1. Results indicate that dispersion may be a useful parameter for assessing fracture risk.

Preliminary investigations of the ultrasonic properties of a bovine cartilage-hydrogel construct have been performed. Results indicate that the reflection coefficient at the cartilage-hydrogel interface may provide a useful measure of integration with the native tissue.

Contributors and Collaborators

A. Slifka (Materials Reliability Division, NIST); K. Anseth (University of Colorado); B. Hoffmeister (Rhodes College of Memphis, TN)

Materials for Electronics

The U.S. electronics industry faces strong international competition in the manufacture of smaller, faster, more functional, and more reliable products. Many critical challenges facing the industry require the continual development of advanced materials and processes. The NIST Materials Science and Engineering Laboratory (MSEL) works closely with U.S. industry covering a broad spectrum of sectors including semiconductor manufacturing, device components, packaging, data storage, and assembly, as well as complementary and emerging areas such as optoelectronics and organic electronics. MSEL has a multidivisional approach, committed to addressing the most critical materials measurement and standards issues for electronic materials. Our vision is to be the key resource within the Federal Government for materials metrology development and will be realized through the following objectives:

- Develop and deliver standard measurements and data;
- Develop advanced measurement methods needed by industry to address new problems that arise with the development of new materials;
- Develop and apply *in situ* as well as real-time, factory floor measurements, for materials and devices having micrometer- to nanometer-scale dimensions;
- Develop combinatorial material methodologies for the rapid optimization of industrially important electronic materials;
- Provide the fundamental understanding of the divergence of thin film and nanoscale material properties from their bulk values;
- Provide the fundamental understanding of materials needed for future nanoelectronic devices, including first principles modeling of such materials.

The NIST/MSEL program consists of projects led by the Metallurgy, Polymers, Materials Reliability, and Ceramics Divisions. These projects are conducted in collaboration with partners from industrial consortia (e.g., International SEMATECH), individual companies, academia, and other government agencies. The program is strongly coupled with other microelectronics programs within the government such as the National Semiconductor Metrology Program (NSMP). Materials metrology needs are also identified through the International Technology Roadmap for Semiconductors (ITRS), the IPC Lead-free Solder Roadmap, the National Electronics Manufacturing Initiative (NEMI) Roadmap, the Optoelectronics Industry Development Association (OIDA) Roadmap, IPC (the International Packaging Consortium), and the National [Magnetic Data] Storage Industry Consortium (NSIC) Roadmap.

In each of these areas, MSEL researchers have made substantial contributions to the most pressing technical challenges facing industry, from new fabrication methods and advanced materials in the semiconductor industry, to advanced packaging materials, to magnetic data storage. Below are just a few examples of MSEL contributions over the past year.

Advanced Gate Dielectrics

To enable further device scaling, the capacitive equivalent thickness (CET) of the gate stack thickness must be 0.5 nm to 1.0 nm. This is not achievable with existing SiO₂/polycrystalline Si gate stacks. Given the large number of possible choices for these new layers, the only feasible approach to understanding the complex materials interactions that result at the gate dielectric/substrate and gate dielectric/metal gate electrode interfaces is through the application of combinatorial methodologies. This same methodology and apparatus are applicable to a wide variety of problems in the electronic materials field.

Sub-100 nm Nanofabrication

The continual decrease in feature size has been the driving force for advances in the semiconductor industry. Current structures have 90 nm dimensions with planned nodes at 65 nm and 35 nm structures. Advanced measurements of the patterning materials (photoresists), are needed to enable future large scale manufacturing of smaller devices. MSEL utilizes advanced x-ray and neutron tools to provide insight into the feasibility and optimization of these important processes.

Advanced Metallization

Electrodeposited copper is rapidly replacing aluminum for on-chip “wiring” because of its lower electrical resistivity, superior electromigration behavior, and the ability to fill fine features without the formation of seams or voids. As feature dimensions go below 100 nm, difficulties in maintaining performance are anticipated. These issues are addressed through a combination of modeling and experimental efforts.

Test Methods for Embedded Passive Devices

Significant advantages arise if passive devices are integrated directly into the circuit board as embedded passive devices rather than discretely attached with automated assembly. New metrology methods were developed to address the needs of the electronic industry. Two test methods were completed and have received wide acceptance by industry as new methods to accelerate the development of embedded passive device technology.

Contact: Robert R. Keller

Electronic Packaging and Components: Packaging Reliability

We are developing methods to examine materials and interfaces in electronic packaging applications and elucidate the damage mechanisms. Our current focus is on advanced packaging structure, embedded passive materials, and thin metal films by use of thermal microscopy to measure heat flow and thermal properties on increasingly smaller size scales.

Andrew J. Slifka

Technical Description

The microelectronics industry is moving toward components of higher density and smaller size that use less expensive materials. One result of this is that reliability becomes an increasing concern due to coefficient of thermal expansion (CTE) mismatch and increased heat flow. As size decreases and functionality increases, thermomechanical fatigue becomes a factor in more areas of the microelectronics industry, including lead-free solders and interconnects.

We are investigating the structural damage induced from CTE mismatches between the various component materials in electronic packages to determine initiation of damage and the ultimate failure mechanisms. Thermal microscopy is used to measure changes in interfacial thermal resistance in order to detect the onset and continuation of thermomechanical damage, leading to electrical failure at interfaces.

We are developing new measurement methods using scanned-probe microscopy (SPM) in order to characterize packages and measure thermal conductivity of thin films at increasingly smaller size scales.

Accomplishments

We have completed measurements on industrial embedded resistors (see Figure 1), making comparative measurements between the SPM thermal system and the IR microscope.

We have made measurements of films by use of thermal SPM in a mode that uses the probe tip simultaneously as a point-source heater and a resistive element in a Wheatstone bridge circuit. For example, we have made preliminary measurements using various thicknesses of gold films on different substrates, and have compared a new theory, developed by our collaborators, to our measurements. Figure 2 shows data from a suite of these measurements. We will add interfacial modifications to the samples and to the theory in order to

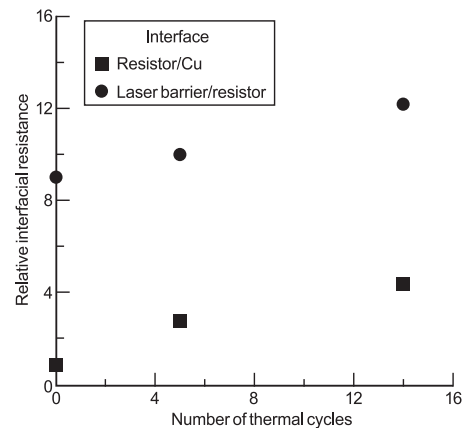


Figure 1: Results of thermal SPM measurements on embedded resistor materials.

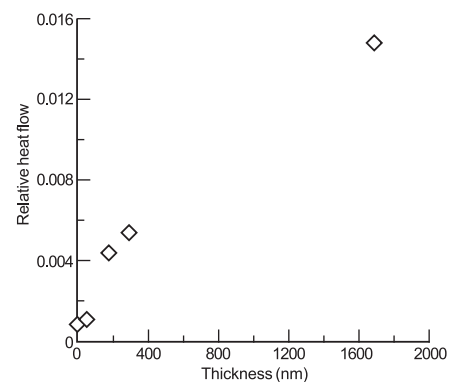


Figure 2: Thermal SPM measurement results on various thicknesses of gold films on glass substrates.

make the measurement method applicable to films used in industry. In addition, we have been using this measurement method on diamond-like-carbon (DLC) films. These industrial films are made from a polymer precursor, which allows easy and inexpensive coating onto various substrates. The thermal conductivity of these films, and how they compare to conventionally processed DLC films, is being investigated.

Finally, we are also measuring thermal conductivity of lead-free solder balls and interfacial thermal resistance between alloys and intermetallics.

Contributors and Collaborators

J. Felten (DuPont Technologies, Research Triangle Park, NC); R. Snogren (SAS Circuits, Inc., Littleton, CO); K. Cole (University of Nebraska, Lincoln, NE); S. Joray (Cenymex Corp., Longmont, CO); F. Hua, (Intel Corp., Santa Clara, CA)

Electronic Packaging and Components: Acoustic Characterization

Bulk acoustic techniques have been developed and applied to the characterization of a variety of materials, with particular emphasis on piezoelectric crystals for electronic oscillator and filter applications. The research includes metrology of mode-selective noncontacting resonant spectroscopy, characterization of physical mechanisms that degrade performance of piezoelectric compounds with the structure of langasite, and determination of elastic constants of body-centered-cubic Ti and the shape-memory alloy NiTi.

**Ward Johnson, Sudook Kim, and
Carlos Martino**

Over the past several decades, the Materials Reliability Division has established special capabilities in a variety of resonant acoustic techniques, including resonant ultrasound spectroscopy (RUS), time-domain resonance methods, noncontacting transduction, Marx-oscillator measurements, and torsional-pendulum measurements. The combined capability of these resonance systems enables elastic constants and anelastic damping to be measured from 4 K to 1100 K. The division also has implemented several conventional pulse-echo systems, including immersion scanning. During FY04, research was focused primarily on noncontacting mode selective metrology, analysis of anelastic damping in piezoelectrics, measurements of the temperature dependence of elastic constants of a shape-memory alloy, and determination of elastic constants of Ti in its high-temperature body-centered-cubic phase.

Langasite ($\text{La}_3\text{Ga}_5\text{SiO}_{14}$) and several of its isomorphs, including langatate ($\text{La}_3\text{Ga}_{5.5}\text{Ta}_{0.5}\text{O}_{14}$), have attracted significant attention in recent years as piezoelectric materials for improved electronic oscillators and filters. Research in our lab over the past year has sought to identify the dominant anelastic mechanisms that degrade the performance of these materials. An algorithm has been developed for fitting the measured temperature and frequency dependences of the mechanical Q to a superposition of loss mechanisms. For langasite, three point-defect relaxations are shown to be superimposed on a contribution that increased monotonically with temperature. In langatate, very similar anelastic effects appear, with distributions of activation energies that apparently arise from variations in residual stress.

To enable robust measurement of elastic constants of trigonal piezoelectric crystals, such as langasite,

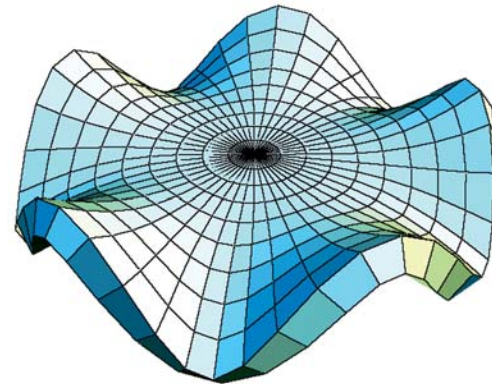


Figure 1: *Vibrational mode of a sapphire disk.*

methods of selectively measuring and analyzing resonant frequencies of modes with specified symmetry have been developed. This approach overcomes errors in analysis that can arise from misidentification of modes. The research has included measurements and analysis of quartz cylinders and sapphire disks. Noncontacting piezoelectric coupling with switchable electrode configurations and Ritz inversion algorithms including full symmetry information have been developed.

In collaboration with Los Alamos National Lab, analysis of resonance measurements on polycrystalline Ti at 1270 K were performed. Polycrystalline elastic constants were determined using the Ritz method. Then, the Kröner model was used to estimate monocrystalline constants from these polycrystalline constants.

Measurements of the temperature dependence of the elastic constants of the shape-memory alloy NiTi have been pursued in collaboration with the Mechanical Engineering Department of the University of Colorado. This study determined the effects of metallurgical treatments on the martensitic transition temperature and elastic constants. Pulse-echo measurements of elastic constants were performed on cold-drawn and hot-rolled specimens from 155 K to 300 K. Large Poisson ratios (> 0.4) reflect the material's superelasticity. Information was obtained on the hysteresis in elastic constants arising from the phase transition, which is a subject of controversy.

Contributors and Collaborators

P. Heyliger (Colorado State Univ.); M. Dunn, K. Gall (Univ. of Colorado, Mechanical Engineering Dept.); H. Ogi (Osaka Univ., Japan); H. Ledbetter (Los Alamos National Lab); A. Teklu (Univ. of Mississippi, Oxford)

Micrometer-Scale Reliability: Mechanical Behavior of Thin Films

Measurement methods and materials data are needed for the design of interconnect structures in high-performance integrated circuits. These micro- and nanometer-scale thin films are formed by physical vapor deposition; their microstructures, and hence their mechanical properties, are quite different from those of bulk materials of the same chemical composition. The ultimate goals of this project are to characterize the exact materials used in IC fabrication, at their proper size scale, and to understand the relevant deformation and failure mechanisms.

David T. Read

Interconnect structures in advanced integrated circuits carry power, signals, and heat from the transistors to the outside environment. These structures consist of multiple layers of thin films of conductors and dielectrics with barrier and adhesive layers. These thin films are an essential component of all advanced electronic devices, and similar materials are used in a variety of other applications, such as reflective coatings. Industry is aggressively pressing new materials into service, reducing the size of the structures, and requiring more functionality, including mechanical functionality, from all components of their structures. Design of reliable structures relies on quantitative numerical modeling, which requires accurate material property data. Because the films are formed by physical vapor deposition, their microstructures, and hence their mechanical properties, are quite different from those of bulk materials of the same chemical composition.

The objectives of this project are:

- To develop experimental techniques to measure the mechanical properties of thin films, in specimens fabricated and sized like materials used in actual commercial devices;
- To relate thin-film mechanical behavior to microstructure;
- To extend test techniques from their present level (1 μm thick, 10 μm wide) to smaller specimens that are similar in size to the conductive traces used in contemporary VLSI circuits (widths of 0.1 to 1 μm).

In previous years we reported properties of aluminum, polyimide, and polysilicon films at room temperature. We have now measured the tensile properties of aluminum films from a commercial source, and lab-made electrodeposited copper films from room temperatures

up to 150 °C. The mechanical properties decline only slightly with increasing temperature, in a pattern normal for face-centered-cubic metals.

Microtensile Young's (elastic) modulus data for nickel were contributed to a comparison study. The microtensile value was 177 ± 8 GPa (most probable uncertainty). Details are given elsewhere, but the conclusion from the full set of measurements is that both the modulus and the density of this sputtered nickel film are lower than bulk values. Microtensile modulus measurements, in particular, have been suspect because the results are often lower, by 10 % or more, than bulk values. See the Molecular Dynamics page of this report for more on this.

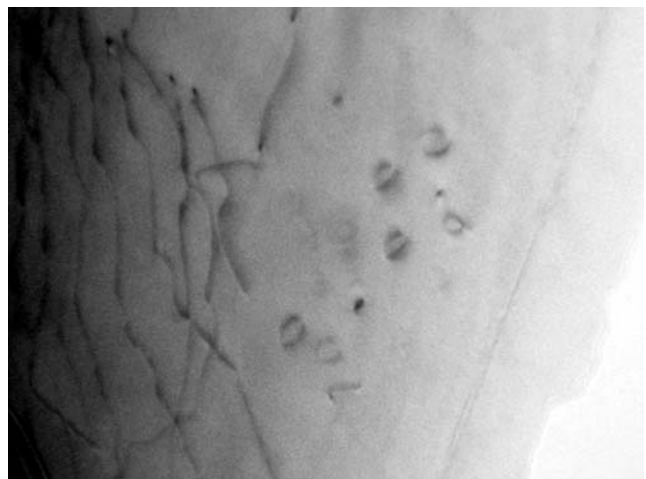


Figure 1: TEM of fractured tether of aluminum contact metal microtensile specimen. The dark lines on the left are dislocations; note their absence toward the right, near the fracture edge.

The transmission electron microscope (TEM) micrograph in Figure 1 shows two different deformation mechanisms for a thin aluminum film. Prismatic vacancy loops, seen as circular features about 20 nm in diameter on the right, are formed in the absence of dislocations in the thinner part of the deformation zone near the fracture edge (far right, lower). Dislocations are seen only in the thicker regions, at the left in the image. The size and density of the loops seems to be dependent on the speed of the deformation, with smaller loops 5–10 nm in diameter seen in more slowly deformed material.

Contributors and Collaborators

Y-W. Cheng, J.D. McColskey, R.R. Keller, R. Geiss, J. Wright (Materials Reliability Division, NIST); MOSIS Service (specimen fabrication)

Micrometer-Scale Reliability: Chip-Level Interconnects

Semiconductor manufacturers require increasingly demanding thermal and electrical performance from chip-level interconnects, as feature sizes continue to shrink. Reliability of such small structures then becomes compromised by failure modes unseen by earlier generation interconnect systems. Our studies address thermal and electrical behaviors of interconnects under conditions of extreme stressing. In particular, we concentrate on the roles of localized stress and variations in micro nanostructure in limiting interconnect performance and lifetime. We performed basic studies on aluminum-based structures undergoing AC stressing at high current density ($>10 \text{ MA/cm}^2$) as well as measurements of electrical behavior in advanced sub-100 nm copper and silver wires.

Robert R. Keller, Roy H. Geiss, and Yi-Wen Cheng

AC stressing at high-current density and low frequencies is used to simulate the thermomechanical fatigue that can occur during a microelectronic device's operational lifetime, due for example to power cycling, energy saving modes, and to application-specific thermal fluctuations. Cyclic Joule heating takes place, leading to differential thermal expansion between metallic interconnects and surrounding substrates or passivation layers. The resulting damage is due to fatigue mechanisms known to operate in bulk metals, but with the constraints associated with thin films imposed. This year, we performed detailed transmission electron microscope (TEM) studies of the deformation mechanisms, supplementing last year's electron backscatter diffraction studies.

Figure 1 shows a pair of TEM images, bright field (above) and weak beam dark field (below), taken from the same region of a cross section of a severely stressed aluminum interconnect. The image shows a high density of dislocation loops, as indicated by arrows. Analysis of diffraction contrast suggests these to be prismatic loops, where the Burgers vector lies normal to the plane of the loop. Such dislocations can be formed by the coalescence of lattice vacancies into a platelike arrangement. Probable sources of vacancies in thermomechanically deformed metal films include grown-in vacancies or those formed during cross-cutting of screw dislocations.

The existence of prismatic loops suggests a possible means for estimating the local temperature rise during a heating cycle. Such loops are known to disappear after prolonged exposure to high temperatures, as vacancies

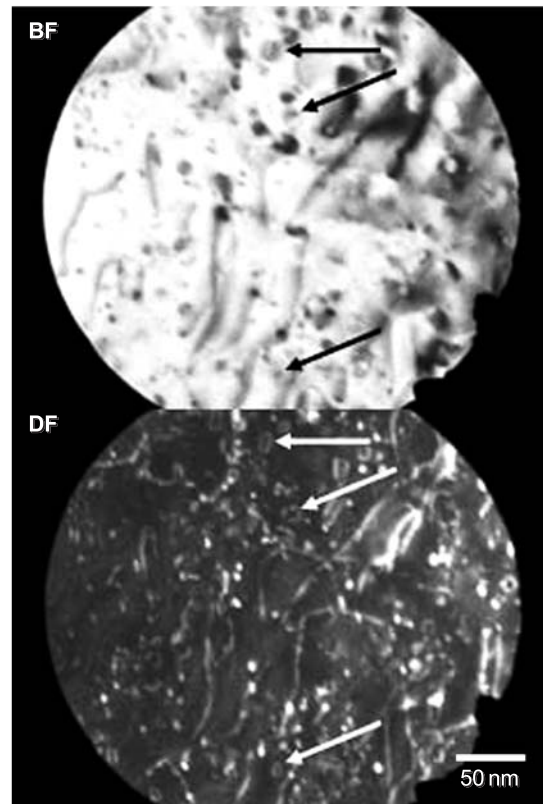


Figure 1: TEM images showing dislocations induced during high-current density AC stressing in aluminum.

diffuse out of the film. The observation of these loops after two hours of testing suggests that there was little sustained exposure above approximately 150°C , which is consistent with our estimates based on electrical resistance measurements. Both a conference proceedings and an archival manuscript are in progress.

We also completed, in collaboration with Metallurgy Division, a study of linewidth effects on resistivity in narrow ($<50 \text{ nm}$) silver interconnects fabricated by patterned electrodeposition. We found that resistivity increases could be attributed to electron scattering from interconnect surfaces. More details are provided in the *Metallurgy Division Annual Report* for fiscal year 2004. A manuscript is now in press for *Journal of Applied Physics*.

Contributors and Collaborators

D. Josell (Metallurgy Division, NIST); C. Burkhard (Clarkson University); C. Witt (Cookson Electronics–Enthone)

Micrometer-Scale Reliability: Dynamic Imaging of Magnetic Domain Walls

The purpose is the development of high-sensitivity, low-noise magnetic sensors for use as metrological tools in health care, homeland security and general information technology. In health care, non-invasive sensors are needed for medical evaluation in the areas of magneto-cardiography and magnetic bead tracking of blood flow and stem cells. In homeland security, sensors are needed to detect low levels of pathogens. In IT, sensors are needed for ND failure analysis and magnetic data storage, among others.

Roy H. Geiss

The goal is to develop multi-level magnetic sensors with a sensitivity better than 1 p-tesla/ $\sqrt{\text{Hz}}$ at 1 Hz noise level that operate at room temperature and can be easily integrated with standard silicon electronics. This involves a many-faceted program that includes materials development, sensor fabrication, sensor characterization, modeling and nanomagnetodynamic imaging. The component being studied here concerns the dynamic observation of magnetic domain walls using Lorentz microscopy in the transmission electron microscope (TEM). Imaging of static magnetic domain walls in the TEM is not new, but our focus is to study the dynamics of domain wall-defect interactions and changes in spin distributions associated with defects or other discontinuities in nanodevices. The ultimate goal is to associate the dynamical interactions with electrical noise measurements in the same sensor.

The effort to image magnetic domain walls has just started. A 200 kV TEM was obtained in 2003. A high-resolution, high-speed CCD camera was installed, and high-resolution, dynamic-magnetic imaging was successfully demonstrated. A sample holder with multiple current feed throughs was designed that allows the application of magnetic fields for *in-situ* testing. Thus far, we have obtained high-resolution images of domain walls at frame rates up to 15 s⁻¹. In particular, we have filmed the formation and movement of Bloch lines and points in cross-tie walls in Ni₈₀Fe₂₀ films 50 nm thick, and have observed the pinning of cross-tie walls at small defects in a noncrystalline CoFeNiSiB alloy film provided by a U.S. magnetic sensor company. Both these dynamic experiments were performed by slowly varying the small local magnetic field in the neighborhood of the specimens in the TEM. Movement of domain walls was possible since the coercivity of both films was very small, on the order of a few oersteds.

The observation of pinning of the domain walls by small defects in the CoFeNiSiB film demonstrated

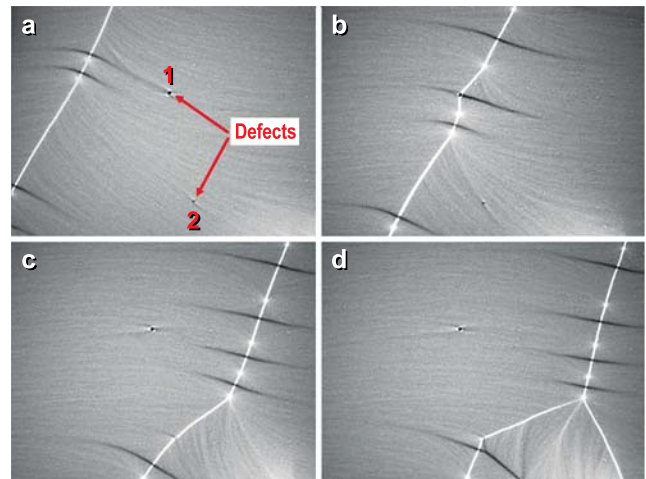


Figure 1: Images *a* to *d* are from a video sequence showing domain wall pinning. The cross-tie wall seen at the left-hand side in *a* slowly moves to the right under the application of a small magnetic field in *b* through *d*. In *b* the wall is pinned by defect 1. With continued applied field, the wall breaks free from defect 1 and moves to defect 2, where it is again pinned, as suggested in *c* and definitely in *d*. Defects 1 and 2 are 4 μm apart.

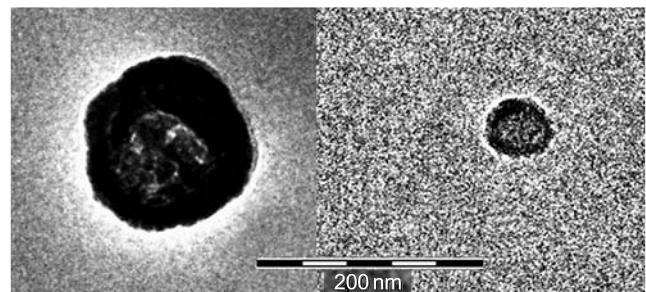


Figure 2: Images of the individual defects 1 and 2.

our capability to view interactions in real time. Further, with frame-by-frame analysis of the video, we determined which defects interacted with the domain walls. A few frames from a video sequence containing domain wall pinning are shown in Figure 1. High magnification images of the noncrystalline defects are given in Figure 2.

An abstract involving this work has been submitted to the “2004 Magnetism and Magnetic Materials” conference. Studies on smaller structures are the next phase.

Contributors and Collaborators

Steve Russek, Bill Rippard, David Pappas (Magnetic Technology Division, NIST)

Micrometer-Scale Reliability: Bridging Length Scales

We have developed a multiscale model for nanostructures in solids. The model relates the physical processes at the interatomic level to measurable lattice distortions at the nanometer level and macroscopic stresses and strains. The model links the subnano (interatomic), nano (nanostructures), and macro length scales by integrating the powerful techniques of molecular dynamics, lattice-statics Green's functions, and continuum Green's functions.

David T. Read and Vinod K. Tewary

Technical Description

Mathematical modeling is a very important tool for understanding the mechanical behavior of nanomaterials and for research and design of devices based upon nanostructures. A nanostructure needs to be modeled at the following scales: (i) the core region of the nanostructure (subnanometer), where the nonlinear effects may be significant; (ii) the region of the host solid around the nanostructure (nanometer); and (iii) free surfaces and interfaces in the host solid (macro). A nanostructure causes lattice distortion in the host solid that manifests as strain throughout the solid. The strain is essentially a continuum-model parameter, whereas the lattice distortions are discrete variables that must be calculated by use of a discrete lattice theory. Hence, one needs a multiscale model that relates the discrete lattice distortions at the microscopic scale to a measurable macroscopic parameter such as strain.

Conventional models of nanostructures are based upon either the continuum theory, which is not valid close to the defect, or molecular dynamics (MD) which is CPU intensive and usually limited to small crystallites, which may introduce spurious size effects. We need a computationally efficient multiscale model that links the length scales from subnano to macro and that can be used on an ordinary desktop. Such a model will be a valuable tool for research and engineering designs.

Our model is based upon the lattice-statics Green's function (LSGF) \mathbf{G} that reduces asymptotically to the continuum Green's function (CGF). The displacement field in this model containing N atoms is given by:

$$\mathbf{u}(\mathbf{l}) = (1/N) \sum_{\mathbf{k}} \mathbf{G}(\mathbf{k}) \mathbf{F}(\mathbf{k}) \exp(i\mathbf{k} \cdot \mathbf{l}),$$

where \mathbf{l} is a lattice site, \mathbf{k} is a reciprocal space vector, and $\mathbf{F}(\mathbf{k})$ is the Kanzaki force, which is calculated by using MD without making the linear approximation.

For small \mathbf{k} , $\mathbf{G}(\mathbf{k})$ reduces to CGF. Thus, for large l , the equation reduces to macroscopic continuum theory while the discrete lattice effects are retained in $\mathbf{F}(\mathbf{k})$. Thus our model is truly multiscale since it seamlessly links the discrete atomistic effects in $\mathbf{F}(\mathbf{k})$ to macroscopic scales through the GF. Even for a million atom model, the calculation of GF takes only a few CPU seconds on a standard 3 GHz desktop.

Accomplishments

Initial conference presentations and a journal paper on this new approach, first reported at the end of FY 2003 and during FY 2004, have been well received.

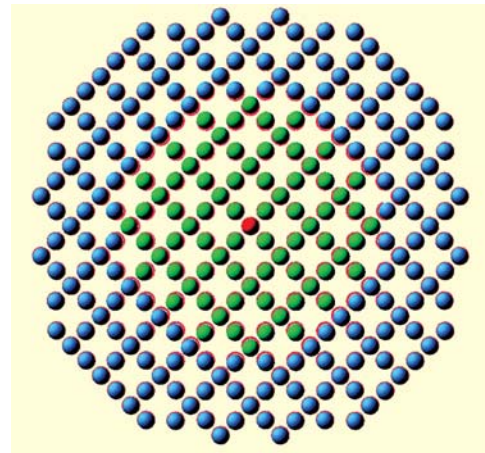


Figure 1: Section through Ge quantum dot in Si matrix after partial relaxation. The red circles indicate the original positions of the Si lattice sites; the atom in red is the center of the QD.

This year, we set out to apply the approach to a more timely, but also more challenging, physical system, namely, a germanium “quantum dot” (QD) in a silicon matrix. On the GF side, the challenge was to treat the more complex diamond-cubic lattice structure; on the MD side, the more complex modified embedded atom model potential, needed for silicon and germanium, had to be coded and tested. As of this writing, the first iteration of the Si-Ge quantum dot is in progress. The figure shows the initial distortions of the diamond cubic lattice around a QD with 281 Ge atoms; the method is capable of handling much larger QD, even with a desktop computer.

Contributors and Collaborators

R.R. Keller, Bo Yang (Materials Reliability Division, NIST); E. Pan (Akron University)

Micrometer-Scale Reliability: Molecular Dynamics

It is widely anticipated that applications of nanomaterials will enable major advances in technology in a variety of fields, including sensors, high-strength materials, medicine, and others. Computer simulations seem to offer a path to quantitative understanding of the behavior of nanoscale materials. The form and parameters of the interatomic forces may turn out to be the most concise and useful representation of materials measurement results. Atomistic simulations are widely used in interpreting nanoscale phenomena at the boundary between mechanics and chemistry and to support the plausibility of proposed devices. We are developing the capability to use molecular-dynamics simulations to interpret our own measurements, and to assess the accuracy of proposed interatomic potentials.

David T. Read

Various approaches to simulating atomic interactions have been reported. The **first-principles** approach uses *quantum mechanical* models of nuclei and electrons. Even though this approach typically includes only the valence electrons, it can handle only a few tens of atoms. Recently, in an innovative study, the first principles approach was used to search for new superalloys.

The **molecular-mechanics** approach, widely used for organic molecules such as proteins, requires explicit assumptions about atomic bonding, specifically, a list of which atoms are bonded to which other atoms. The bonds are represented by force laws, and the configuration of complex molecules can be studied. Different force laws may be used for certain types of atoms, depending on the chemical environment. For instance, the carbon-carbon force law in diamond may be different from that in graphite, because of the difference in local chemistry.

Molecular dynamics (MD) treats atoms or molecules as particles that follow *Newton's laws* of mechanics. The particles interact with a prescribed force law, which depends only on the chemical identity of the interacting atoms. The force laws are derived empirically, and the parameters are selected by fitting to measured properties, such as the elastic constants, the vacancy energy, the energy of sublimation, the phonon frequencies, and others. This approach can treat solids, liquids, or gases, and can model melting temperatures and equilibrium crystal structures.

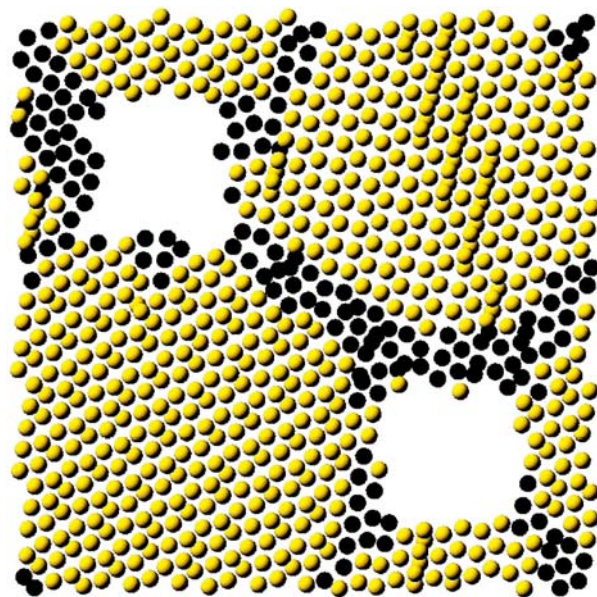


Figure 1: Cross-section from the center of an array of spheres (AS) model. Atoms shown in color have local fcc symmetry. Atoms shown as black have a lower local symmetry. Because of the periodic boundary conditions, this cell is effectively replicated indefinitely in all 3 dimensions.

Molecular-dynamics results obtained in the current fiscal year may indicate a mechanism for the recurring reports that the Young's (elastic) modulus values of thin films are lower than those of the corresponding (perfect) bulk material by 10 % or more. Last year's report showed a high-resolution SEM micrograph of electrodeposited copper with a morphology of agglomerated spheres. Its Young's modulus was over 40 % lower than the bulk value. This year, the elastic behavior of a simplified model of such a solid was simulated by molecular dynamics. Caution is in order. The size scale (number of atoms per sphere) and time scale of the simulation were much less than for the actual specimen. The results, averaged over a random set of crystal directions for the spheres, and for two sizes of spheres, produced a Young's modulus 35 % below the bulk value. This was surprising because continuum-mechanics calculations of the modulus decrease produced by defects of like porosity show values proportional to the volume loss. The present MD results are much more dramatic because after the model was brought to equilibrium, it had a density of about 95 % of the bulk value.

Contributors and Collaborators

J. Rifkin (University of Connecticut, author of MD program used)

Micrometer-Scale Reliability: Solder Reliability

The electronics industry is replacing lead–tin eutectic solders with lead-free solders because of the environmental hazards of lead. In doing so, they have created a need for material property data of the new lead-free solder compositions. A test method has been developed to measure the mechanical properties using specimens on the same size scale as the solder structures used in industry.

Timothy P. Quinn

Background

Industry groups have pointed out the need for material property data for the new lead-free compositions of solder; this includes pooling the data that already exist and filling the critical holes in the data, especially at low-strain rates.

Most of the data that are available for all solders come from specimens that are very large (on the order of millimeters) compared to the solder structures themselves (on the order of hundreds of micrometers). As the solder structures (solder balls for flip chip packages, for example) become smaller ($\sim 150\ \mu\text{m}$), their dimensions approach the dimensions of the phases in the solder itself. The assumption of a homogeneous material used to analyze the stresses in the structure is challenged. We have therefore started testing samples that are on the same size scale as current solder structures to study this interaction.

Accomplishments

A test method that used “miniature” specimens was developed to mimic the size of typical soldered joints. The purpose was to examine the effects of the size of the specimens (and hence the typical structures found in industry) and to fill in the gaps in the data for the lead-free solders. Solder was cast in a Ti mold between two copper blocks, and $300\ \mu\text{m}$ specimens were cut from the blocks. The usable gauge length of the specimens was about $300\ \mu\text{m}$. We can consistently make specimens with a known thermal cycle and maintain well-defined microstructure. Because the samples were sliced off a relatively large “loaf,” a large number of samples could be made in a short time.

After determining the geometry of the gage section using an optical microscope, the specimens were imaged in an ultrasonic microscope with a beam diameter of $45\ \mu\text{m}$ at an operating frequency of 100 MHz.



Figure 1: An ultrasound scan of a solder tensile specimen. The image was made by mapping the amplitude of the reflection off the front interface (white = larger amplitude).

Measuring the time-of-flight from the front to the rear of the sample allowed us to calculate Young’s modulus knowing the density and Poisson’s ratio (Figure 1).

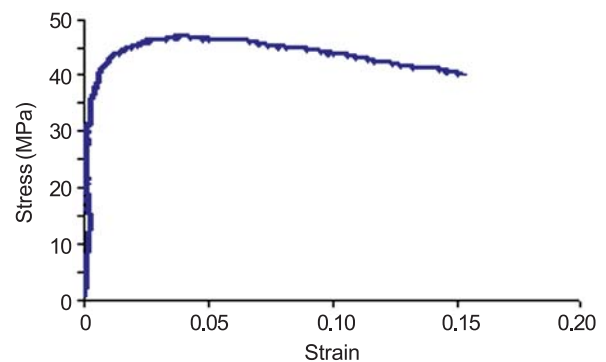


Figure 2: The measured stress–strain curve for a Sn-3.8Ag-0.7Cu solder.

The samples were then tested in uniaxial tension using pin-style grips. The specimens were first painted white, and then a dark line was painted on the specimen over the gauge section. A video-microscope recorded images of the gauge section at about $0.75\ \mu\text{m}/\text{pixel}$. The edges of the gauge section were then tracked with an automated algorithm and used to calculate strain. The stress–strain curve was then plotted (for example see Figure 2). Note that because of the small displacements in the elastic region, the camera does not have enough resolution to adequately predict Young’s modulus. The ultimate tensile strength, yield strength and percent elongation were all obtained using the camera data. Tests have been conducted using Sn-3.8Ag-0.7Cu, Sn-3.7Ag, Sn-0.7Cu, Sn-5Sb, and Sn-37Pb.

Contributors and Collaborators

Ilan Makover, T.P. Quinn, K.R. Waters (Materials Reliability Division, NIST), Yair Rosenthal (Ben-Gurion University, Israel)

Safety and Reliability

While various structural failures have captured national attention over the years, the events of September 11, 2001 generated a greatly increased awareness of vulnerabilities in our national infrastructure. The extent of these vulnerabilities depends to a large degree on the performance of materials in situations outside of the original design considerations. It is now recognized that a critical and urgent national need exists to establish the behavior of materials under such extreme loadings, and to disseminate guidance and tools to assess and reduce future vulnerabilities.

The goal of providing a technical basis for cost-effective changes to national practices and standards, coupled with a need for an integrated effort drawing on capabilities and expertise of a broad collaborative team, has led to the development of the Safety and Reliability Program within MSEL. This program draws on the expertise of several divisions in MSEL and across NIST.

Project selection is guided by an identification and assessment of the particular vulnerabilities within our materials-based infrastructure, and focusing on those issues which would benefit strongly by improved measurements, standards, and materials data. Ultimately, we intend to moderate the effects of acts of terrorism, natural disasters, or other emergencies, all through improved use of materials.

Our vision is to be the key resource within the Federal Government for materials metrology development as realized through the following objectives:

- Identify and address vulnerabilities and needed improvements in U.S. infrastructure
- Develop and deliver standard measurements and data;
- Develop advanced measurement methods needed by industry to address new problems that arise with the development of new materials;
- Support other agency needs for materials expertise.

This program responds both to customer requests (primarily other government agencies) and to the Department of Commerce 2005 Strategic Goal of “providing the information and framework to enable the economy to operate efficiently and equitably.” For example, engineering design can produce safe and reliable structures only when the property data for the materials is available and accurate. Equally importantly, manufacturers and their suppliers need to agree on how material properties should be measured.

The Safety and Reliability Program works toward solutions to measurement problems on scales ranging



from the macro to the micro, in three of the Laboratory’s Divisions (Materials Reliability, Metallurgy, and Polymers). The scope of activities includes the development and innovative use of state-of-the-art measurement systems; leadership in the development of standardized test procedures and traceability protocols; development of an understanding of materials in novel conditions; and development and certification of Standard Reference Materials (SRMs). Many of the tests involve extreme conditions, such as high rates of loading, high temperatures, or unusual environments (*e.g.*, deep underwater). These extreme conditions often produce physical and mechanical properties that differ significantly from the handbook values for their bulk properties under traditional conditions. These objectives will be realized through innovative materials, property measurement and modeling.

The MSEL Safety and Reliability Program is also contributing to the development of test method standards through committee leadership roles in standards development organizations such as the ASTM International and the International Standards Organization (ISO). In many cases, industry also depends on measurements that can be traced to NIST Standard Reference Materials (SRM[®]).

In addition to the activities above, all three divisions provide assistance to various government agencies on homeland security and infrastructural issues. Projects include assessing the performance of structural steels as part of the NIST World Trade Center Investigation, advising the Bureau of Reclamation on metallurgical issues involving pipelines and dams, advising the Department of the Interior on the structural integrity of the U.S.S. Arizona Memorial, and collaborating with both the Department of Transportation and the Department of Energy on pipeline safety issues.

Contact: Thomas A. Siewert or Frank W. Gayle

Infrastructure Reliability: Analysis of Structural Steel in the World Trade Center

In 2002 NIST became the lead agency in the investigation of the World Trade Center collapse. The investigation addresses many aspects of the catastrophe, from occupant egress to factors affecting how long the Twin Towers stood after being hit by the airplanes, with a goal of gaining valuable information for the future. A critical aspect of the investigation is the metallurgical analysis of structural steels from the Twin Towers. The analysis includes characterization of properties, failure modes, and temperature excursions seen by the steel.

**Stephen W. Banovic, Richard J. Fields,
Timothy J. Foecke, William E. Luecke,
J. David McColskey, Christopher N. McCowan,
Thomas A. Siewert, and Frank W. Gayle**

The collapse of the World Trade Center (WTC) Towers on September 11, 2001, was the worst building disaster in human history. Engineers, emergency responders, and the nation were largely unprepared for such a catastrophe. NIST is investigating the disaster (see <http://wtc.nist.gov/>), and a primary objective is to determine why and how the towers collapsed after the initial impact of the aircraft. As part of this investigation, the Metallurgy and Materials Reliability Divisions in MSEL are studying recovered structural steel from the WTC site. Progress in this study is outlined here.

Task 1 — Collect and catalog physical evidence: 236 structural pieces of the WTC towers have been collected, brought to NIST and studied. Reports have been issued documenting the steel, the as-built locations, the structure of the towers based on design documents, and the standards at the time of construction.

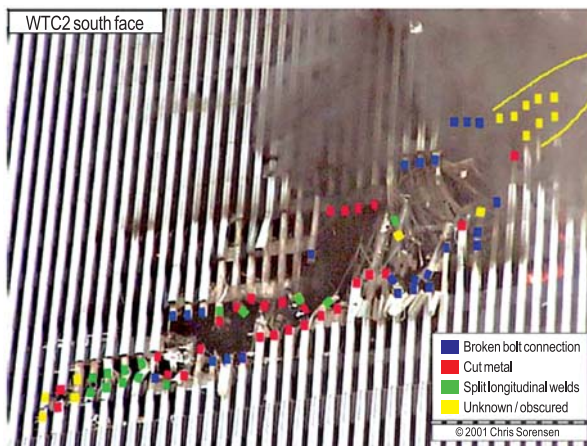


Figure 1: Enhanced image of the impact zone of WTC 2 has allowed determination of failure modes in the perimeter columns.

Task 2 — Categorize failure mechanisms based on visual evidence: Available photographic evidence and recovered steel have been examined and documented as to failure mechanisms (Figure 1).

Task 3 — Determine steel properties to support structure performance and airplane impact modeling studies: 29 different steels have been characterized for room temperature mechanical properties. High-temperature and high-strain-rate tests are now complete. Creep, or time-temperature-dependent behavior, has been determined for floor truss and column steel.

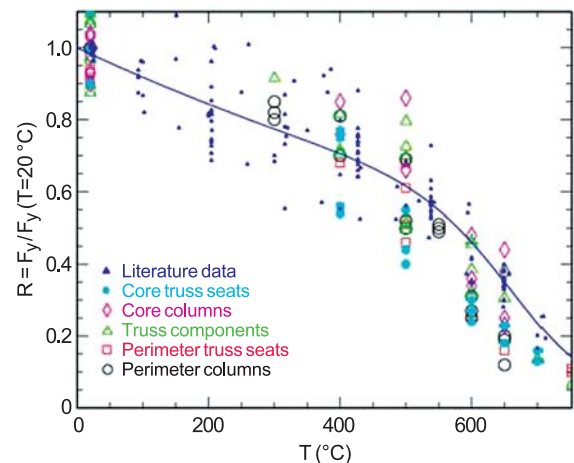


Figure 2: Normalized yield strength and ultimate tensile strength measured as function of temperature. Model curve is based on historical data for WTC era steels.

Task 4 — Correlate determined steel properties with specified properties: Most steel was found to exceed the specified minimum values by 5 to 10 percent.

Task 5 — Analyze steel to estimate temperature extremes: We have developed a technique of paint characterization to provide a quick mapping of temperature excursions seen by the steel. Challenges included deciphering pre- and post-collapse exposure (see related Highlight in this report).

Data on material properties have been provided to aid in the modeling of plane impact and structural response to the fires. A final draft of the investigation report will be released for public comment in December 2004.

Contributors and Collaborators

R. Santoyo, L. Rodine (Materials Reliability Division, MSEL, NIST); M. Williams, S. Claggett, M. Iadicola, R. Jiggetts (Metallurgy Division, MSEL, NIST)

Infrastructure Reliability: Standard Test Methods for Fire-Resistant Steel

The fires in the World Trade Center and the ensuing collapse focused attention on the vulnerability of structural steel to fire. Recently, steel mills in Europe and Japan have begun to market steels designated as “fire-resistant.” This project is developing a standard test method for quantitatively evaluating and comparing the resistance to high-temperature deformation and failure of structural steels.

**William E. Luecke, J. David McColskey,
Richard J. Fields, and Frank W. Gayle**

At room temperature, the stress–strain behavior of structural steel is considered to be independent of time. Above about 300 °C, structural steel begins to lose strength. At still higher temperatures, about 500 °C, creep, or time-dependent deformation, further reduces the load-carrying capability. By 600 °C, most structural steels have lost more than half their strength. For this reason, structural steels in buildings are insulated to minimize the temperature rise and resulting strength loss.

Fire resistant (FR) steels are intended to be drop-in replacements for structural steel. They typically meet the same specifications with similar welding properties and cost only marginally more. Yet these steels retain superior high-temperature strength, offering potential for extra time for building occupants to escape a fire.

In Japan and Europe, FR steels are qualified based on yield strength retention at high temperature. This definition may not be the most appropriate since retained yield strength is a short-time property, yet fire-resistance is often measured in hours. Also, with increasing temperature, strength becomes increasingly sensitive to the strain rate. Current U.S. standards for load-bearing components in fire are based on time to reach a given temperature, so effectively all steels are considered to have the same high-temperature strength reduction, regardless of actual properties.

We are currently studying a hybrid of creep and conventional tension tests. The test specimen is held under constant load as the test temperature ramps upward linearly. Over a narrow temperature range, which can be approximated as a critical temperature, the deformation rate increases dramatically, and the specimen fails. This critical temperature can be used as a measure of fire resistance.

One goal of this project is to refine this test technique and offer it as a draft standard. Published research has established that the temperature ramp test

can rank steels, but definitive studies comparing ordinary and FR steels are lacking. Until a standard test method is developed, it is difficult to confidently compare results between laboratories. This research will focus on understanding the limitations, repeatability, and reproducibility of the method by characterizing several different classes of construction steels. Interlaboratory studies will be used to probe the method’s limitations, precision and bias.

A second goal is to generate constitutive models for modeling high-temperature deformation of steels. If test results are not predictable from underlying deformation behavior, a test cannot possibly indicate real-world performance. A second benefit is that much-needed data will be supplied for finite element modeling of modern structural steel deformation in fire, a prerequisite for performance-based fire resistant design.

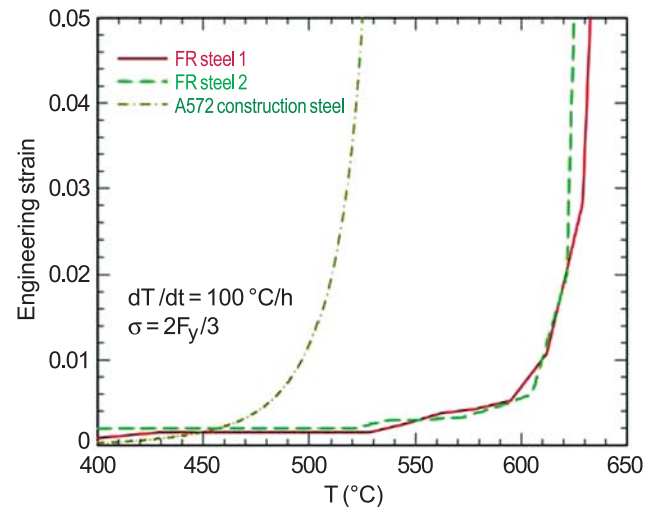


Figure 1: Comparison of “run-away creep” deformation of FR and ordinary construction steel.

Figure 1 illustrates the concept of critical temperature for “run-away” creep for two FR steels and one conventional construction steel. The results demonstrate the potential performance advantage of FR steel. Much more work is necessary, however, to understand the variability in performance of ordinary and FR steels.

During 2004, we also spearheaded the development of an ASTM task group under committee A01 to evaluate test methods for fire resistance of structural steel.

Contributors and Collaborators

M. Bykowski (SURF)

Infrastructure Reliability: Waveform-Based Acoustic Emission

The major project objective is to develop the scientific underpinnings necessary to enhance acoustic emission (AE) technology through increased, high-sensitivity bandwidth. Current secondary objectives include: (1) developing for many users the missing element of modeling AE signals for multiple sources in specimens with and without edge reflections; and (2) developing rational approaches to analyze AE waveforms to solve the real-world problems of reliable identification and location of sources of AE signals.

Thomas A. Siewert and Marvin Hamstad

Technical Description

Acoustic emission (AE) refers to the generation of propagating elastic displacement waves as a result of micro-sized transient-energy releases in a material. Monitoring these waves can provide fundamental information about the location and mechanism(s) of the transient-energy release as well as the time/stress history of such releases. The technical approach, which is beyond that currently commercially offered for either resonant or waveform-based AE technology, is to develop all the key components relevant to a wideband application of AE technology. These include development of wideband high-sensitivity sensor/preamplifiers; high-speed digital recording data-gathering systems of wide dynamic range; finite-element modeling (FEM) to predict near- and far-field displacement waves from AE sources in large and small specimens; wideband experimental AE displacement waveforms from sources in materials of interest; signal-processing techniques to accurately identify source types and their locations; and experimental characterizations of simulated AE wave propagation. The scope in FY2004 covered studies on the effects of electronic background noise on the identification of AE source types through the use of modal amplitudes obtained from wavelet-transform (WT) results.

Accomplishments

Previous work, with FEM-generated signals, demonstrated a technique to identify AE sources by using ratios of modal magnitudes in two different radiation directions. The finite-element code modeled AE signals for dipole-type sources in an aluminum plate 4.7 mm thick. The plate had transverse dimensions sufficient that plate edge reflections did not superimpose on direct signal arrivals. The FEM signals were essentially noise free.

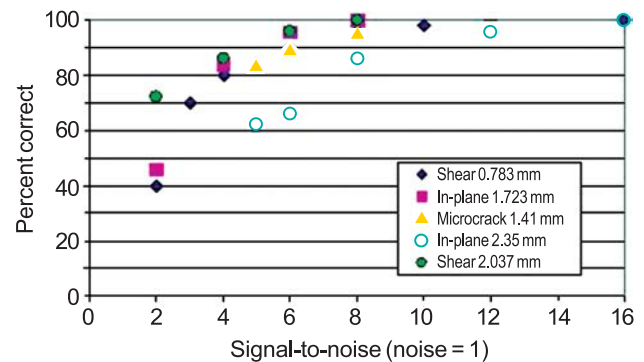


Figure 1: Percent of trials out of 50 with correct source identification versus S/N ratio for the source types and depths listed.

To examine how the presence of electronic noise (from the sensor/preamplifier) alters the ability to correctly identify AE source types, detailed analysis was carried out by superimposing experimental wideband noise on the FEM-based AE signals. Important discoveries were made. The WTs of typical noise signals demonstrated that the WT magnitudes of the noise at each frequency vary with time in a random fashion. Hence, it was necessary to do a statistical study of the effects of noise. Fifty noise segments were prepared. The noise segments were added to the noise-free FEM signals. At each signal-to-noise (S/N) ratio, fifty FEM-plus-noise signals were used for each source type (in-plane dipole, micro-crack initiation, and shear without a moment). The S/N ratio was calculated based on the peak signal amplitude in the assumed direction of applied stress for the three source types. Using the same successful technique for noise free signals, the FEM-plus-noise signals were processed. Figure 1 shows how the number of correct source identifications depends on the S/N ratio. Clearly a S/N ratio of at least six to one is needed to correctly identify a large percentage of the source types. It is expected that all modal amplitude techniques of source identification will be similarly affected. Close examination of the WTs of the noise and the AE signals revealed that the noise signals inhabit the same frequency ranges as the AE signals; hence it will not be straightforward to filter out the noise signals.

Contributors and Collaborators

NIST participants: D. McColskey (Materials Reliability Division, NIST); Cross OU collaborators: A. O'Gallagher, J. Gary (Information Technology Laboratory, NIST); W. Prosser (NASA Langley)

Infrastructure Reliability: Charpy Impact Machine Verification

We assist owners of Charpy impact machines in achieving conformance with the requirements of ASTM Standard E 23. We interact with the ASTM Committee responsible for the Charpy impact standard to improve the service and to maintain a high-quality verification program. We also participate in the activity in ISO Committee TC 164, so our specimens and procedures remain compatible with the associated international and regional standards.

Thomas A. Siewert

Technical Description

The Charpy impact test uses a swinging hammer to assess the resistance of a material to brittle fracture. The absorbed energy is measured from a calibrated scale, encoder, and/or an instrumented striker. The low cost and simple configuration of the test have made it a common requirement in codes for critical structures such as pressure vessels and bridges. This project is handled jointly by the Standard Reference Materials Program (of the Office of Measurement Services), which oversees the administrative aspects of the program, and the Materials Reliability Division, which handles the technical and verification aspects. NIST provides highly characterized standard reference materials (SRMs) to machine owners and independent calibration services, then evaluates the results of tests of these specimens on their impact machines. Owners of machines that meet the requirements of ASTM Standard E 23 are given a letter of conformance, while owners of nonconforming machines are given recommendations on corrective actions. Our special facilities include three master Charpy impact machines (all 300 J to 400 J capacity). These three machines are used to establish certified values for the NIST reference materials sold through the Standard Reference Materials Program Office. In addition, we have several more machines (3 J to 400 J capacities) that are used for research purposes.

Accomplishments

We expect about 950 customers for this service in FY04, a number similar to the customer base in recent years. The great majority of these machines were within tolerances required by ASTM Standard E 23. As usual, many customers took advantage of our support services, as shown by over 674 emails, 730 faxes, and 500 phone

calls in the first 9 months of FY04. We immediately contact the machine owner when it fails to meet the verification criteria. In this contact (by phone, mail, email, or fax), we suggest corrective measures.

One big change this year was that Dan Vigliotti retired after serving as Charpy Coordinator for about 12 years. Ray Santoyo has completed his training for this position and has taken over as Charpy Coordinator. We have just completed a three-year test program that is collecting data on “International Master Batches” of Charpy impact verification specimens. A meaningful harmonization (equivalency) of Charpy V-notch standards around the world is unlikely until the reference materials used for the verification of impact machines in Europe, Japan, and the United States (EN-10045-2, JIS B 7722, and ASTM E 23) share a more common method of certification. The results of this test program are being used to evaluate the use of Master Specimens as a common control in the certification procedure for CVN verification specimens between the three countries’ National Measurement Institutes. It will also evaluate machine variables, offsets, uncertainty, and other factors relevant to the harmonization of our respective systems. Initial results indicate the equivalency of the energy scales used to measure absorbed energy by the United States, Europe, and Japan.

We are helping to organize another international symposium, “Second Symposium on Pendulum Impact Machines: Procedures and Specimens,” to be held in conjunction with the November 2004 meeting of ASTM Committee E 28 in Washington, D.C. Previous symposia have provided valuable insight into improvements in our program.

This year, we dedicated a previous Charpy master machine to Izod impact testing, and expect to produce a new SRM in FY05.

Chris McCowan serves as the Chairman of ISO TC164 SC4 P, on pendulum impact and also as the Chairman of ASTM Subcommittee E28.07 on impact testing.

Contributors and Collaborators

NIST participants: Ray Santoyo (Charpy Program Coordinator), C. McCowan, T. Siewert, J. Clark, D. Cyr, C. Dewald, S. Vincent, N. Neumeyer, J. Percell; External collaborators: IRMM (Europe), NRLM (Japan), Members of ASTM Subcommittee E 28.07

Materials Reliability Division FY04 Annual Report Publication List

Balzar, D., "Characterization of strain by diffraction and its influence on the Curie–Weiss temperature in ferroelectric thin films," *Computer Modeling in Engineering and Sciences*, in press.

Balzar, D., "Size-strain line-broadening analysis of the Ceria round robin: Sample II. The results of the round robin," *J. Appl. Crystallography*, submitted.

Balzar, D., and N.C. Popa, "Elastic-strain tensor and inhomogeneous strain in thin films by x-ray diffraction," *Thin Solid Films* **450**, 29–33 (2004).

Balzar, D., and N.C. Popa, "Residual Strain/Stress and Crystallite Size Modeling in Rietveld Refinement," *Diffraction Analysis of the Microstructure of Materials*, edited by E.J. Mittemeijer and P. Scardi (Springer, 2004) pp. 125–145.

Balzar, D., and N.C. Popa, "Residual Stress Determination by Diffraction: Modeling and Applications," *Proceedings of the International Conference on Computational and Experimental Engineering and Sciences (ICCES'04)*, Tech Science Press, in press.

Cheng, Y.W., D.T. Read, J.D. McColskey, and J.E. Wright, "A tensile-testing technique for micrometer-sized free-standing thin films," *Thin Solid Films*.

Downs, K.S., M.A. Hamstad, and A. O'Gallagher, "Wavelet Transform Signal Processing to Distinguish Different Acoustic Emission Sources," *J. of Acoustic Emission* **21**, 52–69 (2003).

Drexler, E.S., J.E. Wright, A.J. Slifka, C.N. McCowan, D.D. Ivy, and R. Shandas, "Stress-strain behavior of rat pulmonary arteries," *J. Appl. Physiol.*

Drexler, E.S., C.N. McCowan, J.E. Wright, A.J. Slifka, D.D. Ivy, and R. Shandas, "Comparison of strength properties of normotensive and hypertensive rat pulmonary arteries," *Proc. Rocky Mountain Bioengineering Symp.*

Flannery, C., and S. Kim, "Poisson ratio porosity dependence of low k dielectric films," *Appl. Phys. Lett.*

Flannery, C., S. Kim, and D. Hurley, "Opto-acoustic inspection techniques on layered low dielectric constant films for microelectronic interconnect," *Materials Research Society*.

Gall, K., Y. Liu, D. Routkevitch, and D. Finch, "Instrumented microindentation of nanoporous alumina films," *J. Mater. Res.*

Gall, K., G. Stafanic, D. Balzar, M.L. Dunn, and Y. Liu, "Internal stress storage in shape memory polymer nanocomposites," *Appl. Phys. Lett.* **85** 290–292 (2004).

Hamstad, M.A., K.S. Downs, and A. O'Gallagher, "Practical Aspects of Acoustic Emission Source Location by a Wavelet Transform," *J. of Acoustic Emission* **21**, 70–94, A1–A7 (2003).

Hartman, A.B., P. Rice, D.S. Finch, G.D. Skidmore, and V.M. Bright, "Force-deflection characterization of individual carbon nanotubes attached to MEMS devices," *Proc. Actuators and Sensors, MEMS 2004 Conf.*

Heyliger, P., S. Cook, W. Johnson, and S. Kim, "Continuum-based free vibration of circular elastic and piezoelectric trigonal plates," *J. of Sound and Vibration*.

Hurley, D.C., and J.A. Turner, "Humidity effects on the determination of elastic properties by atomic force acoustic microscopy," *J. Appl. Phys.* **95**, 2403 (2004).

Hurley, D.C., K. Shen, N.M. Jennett, and J.A. Turner, "Atomic force acoustic microscopy methods to determine thin-film elastic properties," *J. Appl. Phys.* **94**, 2347 (2003).

Johnson, W.L., S.A. Kim, and S. Uda, "Acoustic loss in langasite and langanite," *Proceedings of the 2003 IEEE International Frequency Control Symposium*, p. 646 (2003).

Josell, D., C. Burkhard, Y. Li, Y.W. Cheng, R.R. Keller, C.A. Witt, D.R. Kelley, J.E. Bonevich, B.C. Baker, and T.P. Moffat, "Electrical properties of superfilled sub-micrometer silver metallizations," *Journal of Applied Physics* **96** (1), July 2004.

Keller, R.R., R. Geiss, Y.W. Cheng, and D.T. Read, "Microstructure evolution during alternating-current-induced fatigue," *2004 ASME International Mechanical Engineering Congress*, Nov. 13–19, (2004) Anaheim, CA.

Ledbetter, H., H. Ogi, S. Kai, S. Kim, and M. Hirao, "Titaniums b.c.c. monocrystal elastic constants," *J. Appl. Phys.*

Lomonosov, M., P. Hess, R.E. Kumon, and M.F. Hamilton, "Laser-generated nonlinear surface wave pulses in silicon crystals," *Phys. Rev. B* **69**, 035314 (2004).

Miller, D., C. Hermann, K. Spark, D. Finch, S. George, C. Stoldt, and K. Gall, "Thermomechanical behavior and reliability of Au/Si MEMS structures," *Intl. Reliability Phys. Forum*.

Padilla, T.M., J.R. Berger, D.R. Munoz, T.P. Quinn, and R.A.L. Rorrer, "Contact models of GMAW wire liner friction: An inverse photoelastic solution," Proc. 85th Annual AWS Convention and 2004 Welding Show.

Popa, N.C., D. Balzar, G. Stefanic, S. Vogel, D. Brown, M. Bourke, and B. Clausen, "Residual-strain determination by least-squares refinement of TOF neutron-diffraction measurements of deformed uranium," *Advances in X-Ray Analysis*, 47 (2004) CD-ROM.

Quinn, T.P., T.L. Oreskovic, C.N. McCowan, and N.R. Washburn, "Material models for a poly(ϵ -caprolactone) scaffold," *Proc., 41st Ann. Rocky Mountain Bioengineering Symp.*

Read, D.T., "Atomistic simulation of modulus deficit in thin film copper electrodeposits," *J. Appl. Phys.*

Read, D.T., R. Geiss, and Y.W. Cheng, "Morphology, microstructure, and mechanical properties of a copper electrodeposit," *Microelectronic Engineering*.

Read, D.T., R. Geiss, and Y.W. Cheng, "Mechanical behavior of electrodeposited copper film at elevated temperatures," *2004 ASME International Mechanical Engineering Congress*, Nov. 13–19, 2004, Anaheim, CA.

Rice, P., R.H. Geiss, A.B. Hartman, and S.E. Russek, "Practical application of electron beam deposition welding to building carbon nanotube devices," Proc. Amer. Vacuum Soc. 5th Intl. Conf. on Microelectronics and Interfaces.

Rice, P., R.H. Geiss, S.E. Russek, A.B. Hartman, and D.S. Finch, "Electron Beam Deposition Welding: A Practical Application to Building Carbon Nanotube Devices," *Journal of Vacuum Science and Technology B*, submitted.

Rorrer, R.A.L., A.J. Slifka, H.V. Panchawagh, D.S. Finch, and R.L. Mahajan, "Calibration of vertically actuated MEMS devices via the AFM," *J. Microelectromechanical Systems*.

Shen, K., D.C. Hurley, and J.A. Turner, "Dynamic behavior of dagger-shaped atomic force microscope cantilevers," *Nanotechnology*, submitted.

Siewert, T.A., and W. Rippey, "Thirteenth International Conference on Computer Technology in Welding," *NIST SP 1008*.

Siewert, T.A., and C.N. McCowan, "The Development of Procedures for Impact Testing," *Journal of ASTM International*, submitted.

Slifka, A.J., H. Panchawagh, R.L. Mahajan, D. Finch, and R.A.L. Rorrer, "Static and quasi-static calibration of a bio-MEMS device," *Proc., 41st Ann. Rocky Mountain Bioengineering Symp.*

Slifka, A.J., E.S. Drexler, J.E. Wright, and R. Shandas, "Bubble-test method for synthetic and bovine vascular material," *J. Biomech.*

Slifka, A.J., H.V. Panchawagh, R.A.L. Rorrer, R.L. Mahajan, and D.S. Finch, "Force and displacement calibration of a bio-MEMS device," *J. Microelectromech. Syst.*

Splett, J.D., and C.N. McCowan, "Summary of Charpy Impact Verification Data: 1993–2003," BERB JULY XX).

Sundaram, V., R.L. Mahajan, D.S. Finch, and S.A. Hooker, "Thermal, electrical, and mechanical characterization of carbon nanotube-epoxy composites," *Proceedings of ASME HT-FED 2004*, July 11–15, 2004, Charlotte, NC.

Tewary, V.K., and D.T. Read, "Integrated Green's function molecular dynamics method for multiscale modeling of nanostructures: Application to Au nanoisland in Cu," *CMES (Computer Modeling in Engineering and Science)*.

Tewary, V.K., "Green's function method for modeling surface acoustic wave dispersion in anisotropic material systems and determination of material parameters," *Wave Motion*.

Tewary, V.K., "Elastostatic Green's function for advanced materials subject to surface loading," *J. Eng. Math.*

Tewary, V.K., and D.T. Read, "Multiscale modeling of quantum nanostructures using integrated Greens function and molecular dynamics," *Pre-conf. Proc. ICCES 04*, July 26–29, 2004.

Tewary, V.K., and D.T. Read, "Multiscale Green's function method for modeling quantum nanostructures" *Proc. 12th International Workshop on Physics of Semiconductor Devices*, edited by K.N. Bhat and A. Das Gupta, 1, 521–526 (2003).

Tewary, V.K., "Multiscale Green's-function method for modeling point defects and extended defects in anisotropic solids: application to a vacancy and free surface in copper," *Physical Review B* **69** 094109 (2004).

Turner, J.A., and D.C. Hurley, "Ultrasonic methods in contact atomic force microscopy," *Ultrasonic Methods for Material Characterization*, edited by D. Placko and T. Kundu (Paris: Hermes Science Publications, 2003), Chap. 5, 117–148.

Waters, K.R., J. Mobley, and J.G. Miller, "Causality-imposed (Kramers–Krönic) relationships between attenuation and dispersion: Historical perspective," *IEEE Trans. Ultrason. Ferroelect. Freq. Cont.*

Wright, J.E., E.S. Drexler, A.J. Slifka, C.N. McCowan, D.D. Ivy, and R. Shandas, "Estimation of stress and strain in rat pulmonary artery material during a biaxial bubble test," *Proc. Rocky Mountain Bioengineering. Symp.*, April 23–25, (2004).

Yang, B., and V.K. Tewary, "Defect Greens function analysis of an inhomogeneous quantum dot in a half-space anisotropic substrate," *J. Appl. Phys.*

Yang, B., E. Pan, and V.K. Tewary, "Three-dimensional Green's function of steady-state motion in anisotropic half-space and bimerials," *Engineering Analysis with Boundary Elements*, (2004).

Yang, B., and V.K. Tewary, "Continuum Dyson's equation and defect Green's function in a heterogeneous anisotropic solid," *Mechanics Research Communications* **31**, 405–414 (2004).

Yang, B., and V.K. Tewary, "Static responses of a multilayered anisotropic piezoelectric structure to point force and point charge," *Smart Materials and Structures* **13**, 175–183 (2004).

Materials Reliability Division

Chief

Alan F. Clark

Phone: 303-497-5202

E-mail: aclark@boulder.nist.gov

Deputy Chief

Thomas A. Siewert

Phone: 303-497-3523

E-mail: siewert@boulder.nist.gov

Group Leaders

Microscale Measurements

Robert R. Keller

Phone: 303-497-7651

E-mail: keller@boulder.nist.gov

Microstructure Sensing

Stephanie A. Hooker

Phone: 303-497-4326

E-mail: shooker@boulder.nist.gov

Process Sensing & Modeling

Thomas A. Siewert

Phone: 303-497-3523

E-mail: siewert@boulder.nist.gov

Research Staff

Cheng, Yi-Wen

cheng@boulder.nist.gov
Deformation and strain
Scanning electron microscopy
Microstructural characterization

Drexler, Elizabeth

drexler@boulder.nist.gov
Electron-beam moiré
Tissue mechanics
Metrology of biomaterials

Geiss, Roy

geiss@boulder.nist.gov
Electron microscopy
Microstructural characterization
Materials science

Hamstad, Marvin

hamstad@boulder.nist.gov
Acoustic emission
Composite materials
Nondestructive evaluation

Hooker, Stephanie

shooker@boulder.nist.gov
Nanomaterials and composites
Electromechanical characterization
Sensors and actuators

Hurley, Donna C.

hurley@boulder.nist.gov
Microscale elasticity
Nonlinear ultrasonics
Solid-state physics

Johnson, Ward

johnson@boulder.nist.gov
Ultrasonic measurements
Internal friction
Process sensing

Keller, Robert

keller@boulder.nist.gov
Materials science
Electron microscopy
Mechanical behavior

Kim, Sudook

sak430@boulder.nist.gov
Elastic properties
Low-temperature physical properties
Ultrasonic measurements

McColskey, J. David

mccolske@boulder.nist.gov
Crack propagation
Composite materials
Mechanical testing

McCowan, Christopher

mccowan@boulder.nist.gov
Charpy impact testing
Microscopy and failure analysis
Metrology of biomaterials

Oreskovic, Tammy

oreskov@boulder.nist.gov
Metrology of biomaterials
Scaffold materials
Mechanical measurements

Quinn, Timothy

quinn@boulder.nist.gov
Metrology of biomaterials
Modeling of biomaterials
Strength of lead-free solders

Read, David

read@boulder.nist.gov
Electronic packaging
Elastic-plastic fracture mechanics
Mechanical behavior of thin films

Rice, Paul

paulrice@boulder.nist.gov
Scanned probe microscopy
Magnetic force microscopy
Nanometer scale manipulation

Rodine, Lonn

rodine@boulder.nist.gov
Instrumentation
Data collection and reduction
Computer support

Santoyo, Raymond

santoyo@boulder.nist.gov
Instrumentation
Charpy impact testing
Computer support

Siewert, Thomas

siewert@boulder.nist.gov
Standard reference materials
X-ray sensing and diffraction
Weld sensing

Slifka, Andrew

slifka@boulder.nist.gov
Thermal conductivity
Thermal barrier coatings
Surface characterization

Tewary, Vinod

tewary@boulder.nist.gov
Solid-state physics
Green's-function methods
Elastic-wave propagation

Waters, Kendall

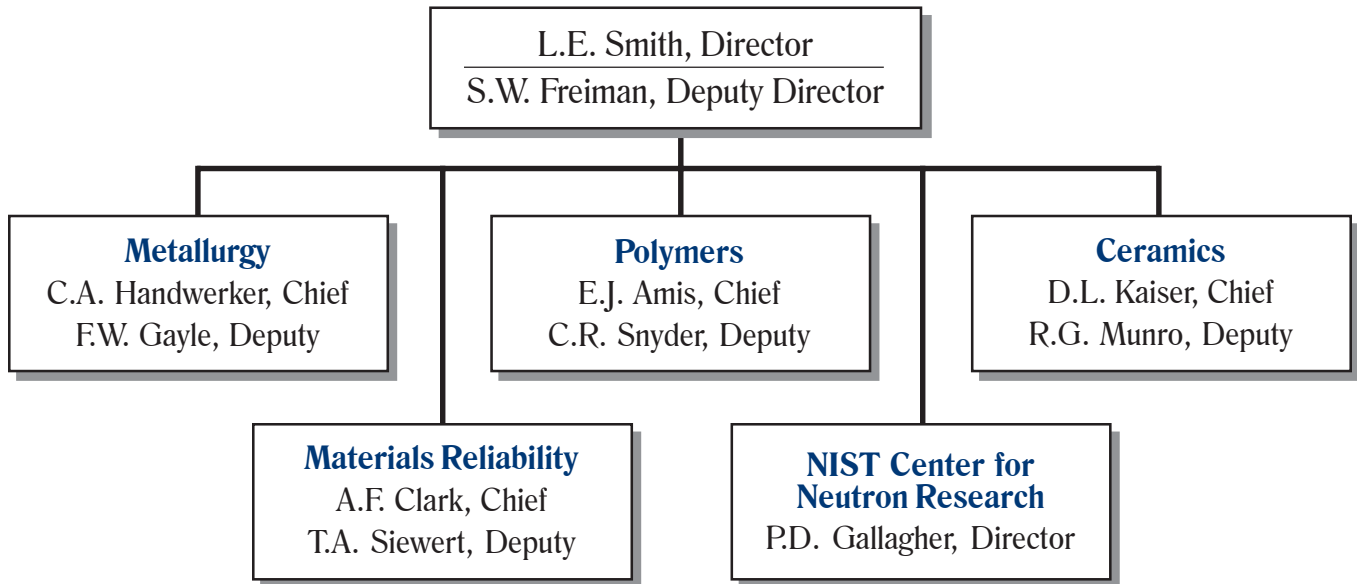
krwaters@boulder.nist.gov
acoustic microscopy
ultrasonic biomaterial evaluation
wave propagation and scattering

Wright, Joyce

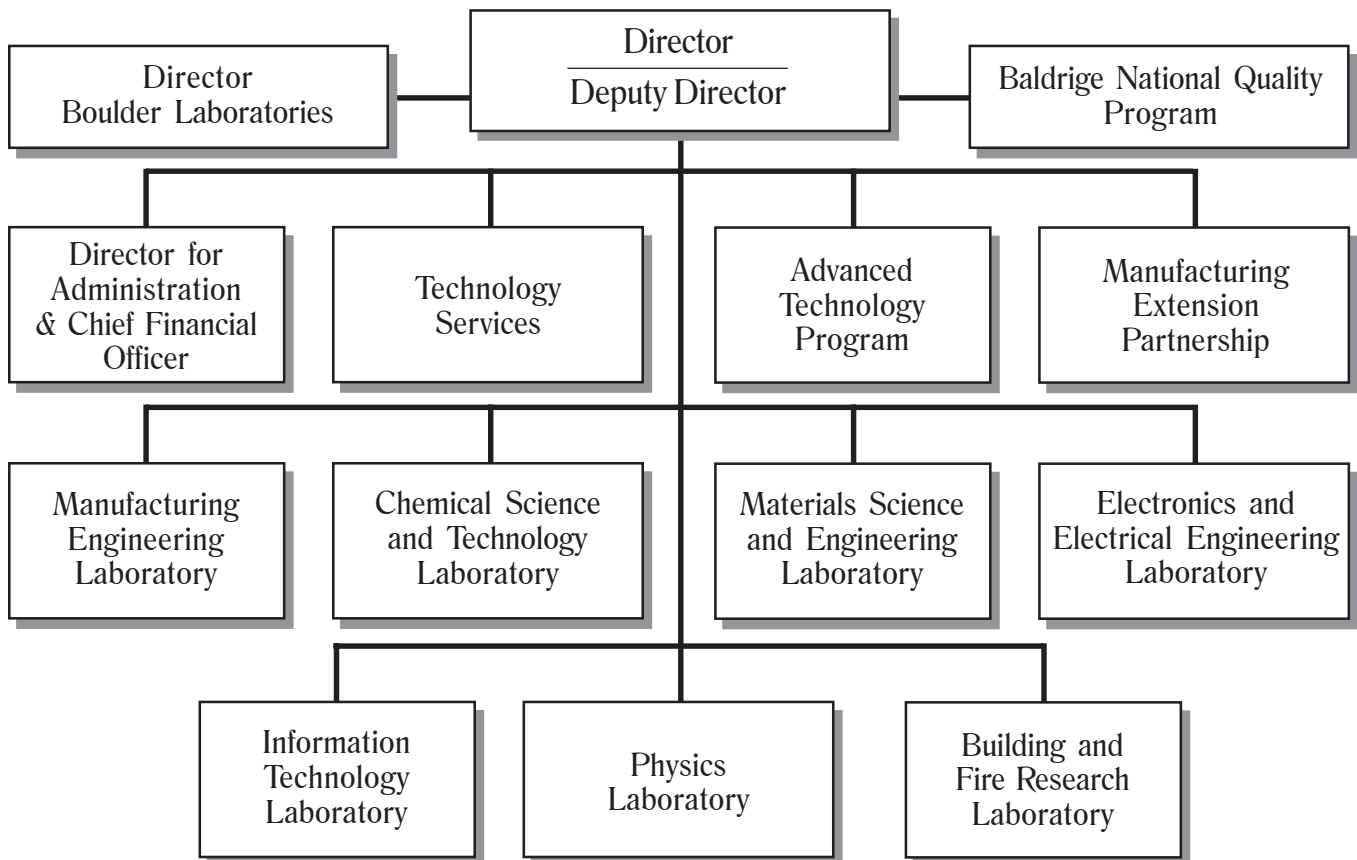
jewright@boulder.nist.gov
Modeling of material behavior
Finite-element analysis
Mechanical behavior of thin films

Organizational Charts

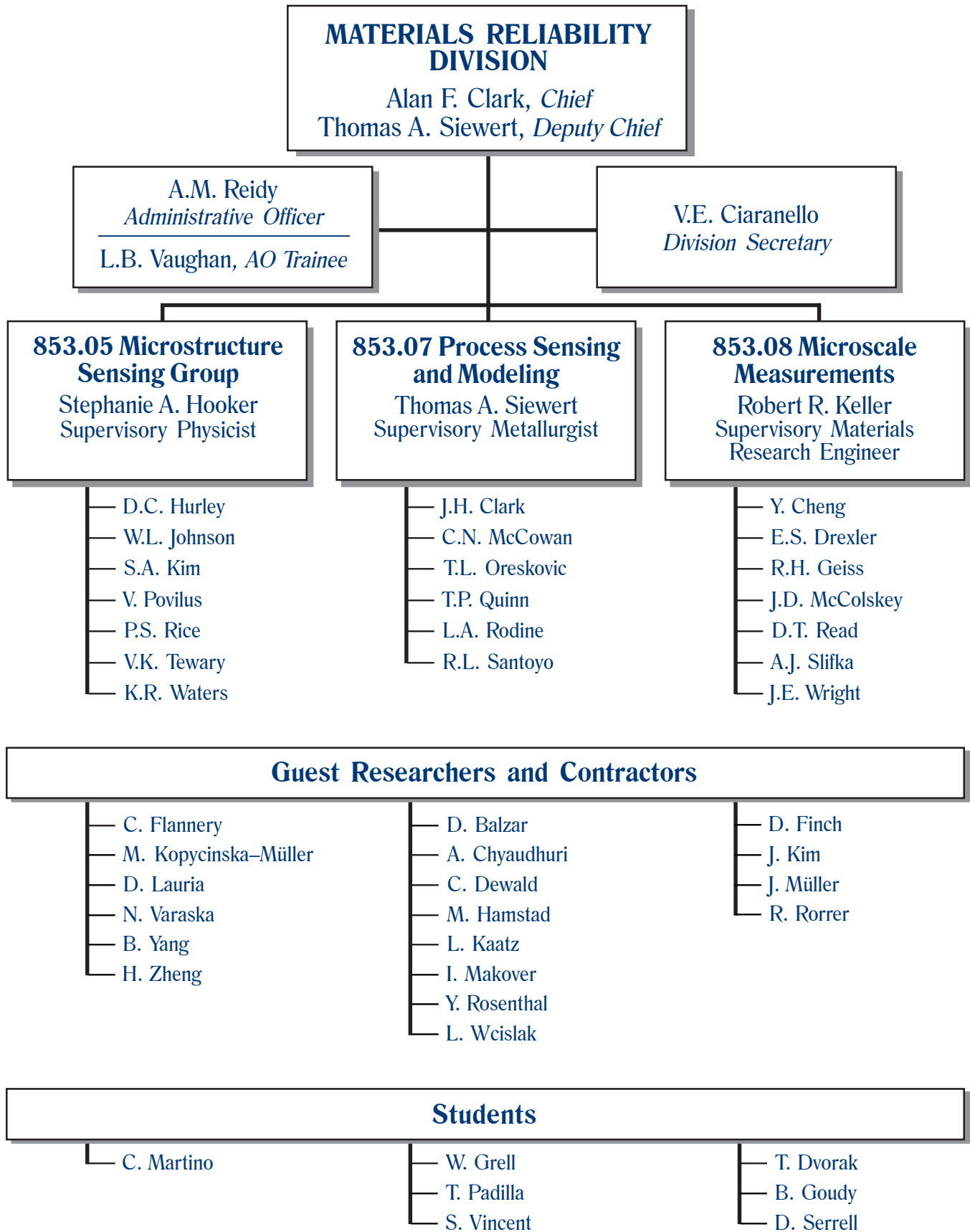
Materials Science and Engineering Laboratory



National Institute of Standards and Technology



Materials Reliability Division (853.00) Organization Chart — 2004



NLST

